Earth Syst. Sci. Data, 17, 1075–1100, 2025
https://doi.org/10.5194/essd-17-1075-2025

Open Access Earth System Science Data

An updated synthesis of ocean total alkalinity and dissolved inorganic carbon measurements from 1993 to 2023: the SNAPO-CO_2-v2 dataset

Nicolas Metzl[1], Jonathan Fin[1,2,a], Claire Lo Monaco[1], Claude Mignon[1], Samir Alliouane[3], Bruno Bombled[4], Jacqueline Boutin[1], Yann Bozec[5], Steeve Comeau[3], Pascal Conan[6,7], Laurent Coppola[3,7], Pascale Cuet[8], Eva Ferreira[4], Jean-Pierre Gattuso[3,9], Frédéric Gazeau[3], Catherine Goyet[10], Emilie Grossteffan[11], Bruno Lansard[4], Dominique Lefèvre[12], Nathalie Lefèvre[1], Coraline Leseurre[13], Sébastien Petton[14], Mireille Pujo-Pay[7], Christophe Rabouille[4], Gilles Reverdin[1], Céline Ridame[1], Peggy Rimmelin-Maury[11], Jean-François Ternon[15], Franck Touratier[10], Aline Tribollet[1], Thibaut Wagener[12], and Cathy Wimart-Rousseau[16]

[1]Laboratoire LOCEAN/IPSL, Sorbonne Université-CNRS-IRD-MNHN, 75005 Paris, France
[2]OSU Ecce Terra, Sorbonne Université-CNRS, 75005 Paris, France
[3]Sorbonne Université, CNRS, Laboratoire d'Océanographie de Villefranche, LOV, 06230 Villefranche-sur-Mer, France
[4]Laboratoire des Sciences du Climat et de l'Environnement, LSCE/IPSL, UMR 8212 CEA-CNRS-UVSQ, Université Paris-Saclay, 91191 Gif-sur-Yvette, France
[5]Station Biologique de Roscoff, UMR 7144 – EDYCO-CHIMAR, Roscoff, France
[6]Sorbonne Université, CNRS, Laboratoire d'Océanographie Microbienne, LOMIC, 66650 Banyuls-sur-Mer, France
[7]Sorbonne Université, CNRS OSU STAMAR – UAR2017, 4 Place Jussieu, 75252 Paris, France
[8]Laboratoire ENTROPIE and Laboratoire d'Excellence CORAIL, Université de La Réunion-IRD-CNRS-IFREMER-Université de la Nouvelle-Calédonie, 97744 Saint-Denis, Réunion, France
[9]Institute for Sustainable Development and International Relations, Sciences Po, 27 rue Saint Guillaume, 75007 Paris, France
[10]Espace-Dev UMR 228 Université de Perpignan Via Domitia, IRD, UM, UA, UG, 66860 Perpignan, France
[11]Institut Universitaire Européen de la Mer (OSU-IUEM), Univ Brest, CNRS-UAR3113, 29280 Plouzané, France
[12]Aix Marseille Univ, Université de Toulon, CNRS, IRD, MIO, Marseille, France
[13]Flanders Marine Institute (VLIZ), 8400 Ostend, Belgium
[14]Ifremer, Univ Brest, CNRS, IRD, LEMAR, 29840 Argenton, France
[15]MARBEC, Univ Montpellier, CNRS, Ifremer, IRD, Sète, France
[16]National Oceanography Centre Southampton, European Way, Southampton, SO14 3ZH, UK
[a]now at: Institut des Sciences de la Terre, 38058 Grenoble, France

Correspondence: Nicolas Metzl (nicolas.metzl@locean.ipsl.fr)

Received: 11 October 2024 – Discussion started: 5 November 2024
Revised: 14 January 2025 – Accepted: 22 January 2025 – Published: 14 March 2025

Abstract. Total alkalinity (A_T) and dissolved inorganic carbon (C_T) in the oceans are important properties to understand the ocean carbon cycle and its link with global change (ocean carbon sinks and sources, ocean acidification) and ultimately to find carbon-based solutions or mitigation procedures (marine carbon removal). We present an extended database (SNAPO-CO_2; Metzl et al., 2024c) with 24 700 new additional data for the period 2002 to 2023. The full database now includes more than 67 000 A_T and C_T observations along with

Published by Copernicus Publications.

basic ancillary data (time and space location, depth, temperature, and salinity) in various oceanic regions obtained since 1993 mainly in the framework of French research projects. This includes both surface and water columns data acquired in open oceans, coastal zones, rivers, the Mediterranean Sea, and either from time series stations or punctual cruises. Most A_T and C_T data in this synthesis were measured from discrete samples using the same closed-cell potentiometric titration calibrated with certified reference material, with an overall accuracy of $\pm 4\,\mu mol\,kg^{-1}$ for both A_T and C_T. The same technique was used on board for underway measurements during cruises conducted in the southern Indian and Southern oceans. The A_T and C_T data from these cruises are also added to this synthesis. The data are provided in one dataset for the global ocean (https://doi.org/10.17882/102337, Metzl et al., 2024c) that offers a direct use for regional or global purposes, e.g., A_T–salinity relationships, long-term C_T estimates, constraint and validation of diagnostics C_T and A_T reconstructed fields, ocean carbon and coupled climate–carbon models simulations, and data derived from Biogeochemical Argo (BGC-Argo) floats. These data can also be used to calculate pH, fugacity of CO_2 (fCO_2), and other carbon system properties to derive ocean acidification rates or air–sea CO_2 fluxes.

1 Introduction

The ocean plays a major role in reducing the impact of climate change by absorbing more than 90 % of the excess heat in the climate system (Cheng et al., 2020, 2024; von Schuckmann et al., 2023; IPCC, 2022) and about 25 % of anthropogenic CO_2 (Friedlingstein et al., 2022, 2023). In the last decade, the oceans have experienced a rapid warming, the year 2023 being the hottest since 1955 (Cheng et al., 2024). In the atmosphere the CO_2 concentration continues its terrific progressive rise, reaching 419.3 ppm in 2023 (a rate of $+2.83\,ppm\,yr^{-1}$; Lan et al., 2024). In August 2024, the global atmospheric CO_2 concentration was already above 420 ppm. In the next decade the oceans will continue to capture heat and CO_2, somehow limiting the climate change, but this oceanic CO_2 uptake changes the chemistry of seawater, reducing its buffering capacity (Revelle and Suess, 1957; Jiang et al., 2023). This process, known as ocean acidification, has potential impacts on marine organisms (Fabry et al., 2008; Doney et al., 2009, 2020; Gattuso et al., 2015). With atmospheric CO_2 concentrations, surface ocean temperature and ocean heat content, sea level, sea ice, and glaciers, ocean acidification (decrease in pH) is now recognized by the World Meteorological Organization as one of the seven key properties of global climate indicators (WMO/GCOS, 2018). Ocean acidification is specifically referred to in the Sustainable Development Goal 14.3.1 Indicator, coordinated at the Intergovernmental Oceanographic Commission (IOC) of UNESCO. Observing the carbonate system in the open oceans, coastal zones, and marginal seas and understanding how this system changes over time are thus highly relevant not only to quantify the global ocean carbon budget, the anthropogenic CO_2 inventories, or ocean acidification rates, but also to understand and simulate the processes that govern the complex CO_2 cycle in the ocean (e.g., Goyet et al., 2016, 2019) and to better predict the future evolution of climate and global changes (Eyring et al., 2016; Kwiatkowski et al., 2020; Jiang et al., 2023). As the rate of change in ocean acidification presents large temporal and regional variability, long-term observations are required. Weekly to monthly regular resolution data are needed to better investigate the long-term change in the carbonate system in regions subject to extreme events (e.g., tropical cyclones, marine heat or cold waves, rapid freshening, convection, dust events, river discharges). In this context it is recommended to progress in data synthesis of the ocean carbon observations that would offer new high-quality products for the community (e.g., for GOA-ON, https://www.goa-on.org, last access: 22 January 2025, IOC/SDG 14.1.3, https://oa.iode.org/, last access: 22 January 2025; Tilbrook et al., 2019).

In this work, following the first SNAPO-CO_2 synthesis product (Metzl et al., 2024a), we present a new synthesis of more than 67 000 A_T and C_T data, measured either on the shore or on board research vessels obtained over the 1993–2023 period during various cruises or at time-series stations mainly supported by French projects. Hereafter this new dataset will be cited as SNAPO-CO_2-v2. The methods, data assemblage, and quality control were presented in version V1. Here, we describe the new data added and discuss some potential uses of this dataset.

2 Data collection

The time series projects and research cruises from which new data were collated are listed in Table 1 with information and references in the Supplement (Tables S1, S3, and S4). The sampling locations of new data are displayed in Fig. 1 (the locations for all data are presented in Fig. S1 in the Supplement). Sampling was performed either from CTD/rosette casts (Niskin bottles) or from the ship's seawater supply (intake at about 5 m depth depending on the ship and swell). Samples collected in 500 mL borosilicate glass bottles were poisoned with 100 to 300 µL of $HgCl_2$ depending on the cruises, closed with greased stoppers (Apiezon®) and held tightly using elastic bands following the SOP protocol (DOE, 1994; Dickson et al., 2007). Some samples

were also collected in 500 mL bottles closed with screw caps. After completion of each cruise, most of discrete samples were returned back to the LOCEAN laboratory (Paris, France) and stored in a dark room at 4 °C before analysis, generally within 2–3 months after sampling (sometimes within a week). In this version we added data from samples that were also returned to University of Perpignan or to University of Réunion. In addition to the discrete samples analyzed for various projects conducted mainly in the North Atlantic, tropical Atlantic, Mediterranean Sea, and coastal regions (Table 1), we complemented this second synthesis with A_T and C_T surface observations obtained in the Indian and Southern oceans during the OISO cruises in 2019–2021 (Leseurre et al., 2022; Metzl et al., 2022; data also available at NCEI–OCADS: https://www.nodc.noaa.gov/ocads/oceans/VOS_Program/OISO.html, last access: 22 January 2025) and MINERVE cruises in 2002–2018 (Laika et al., 2009; Brandon et al., 2022). The A_T and C_T measurements from the MINERVE cruises were performed either on board R/V *Astrolabe* or back in the laboratories (at LOCEAN laboratory and at University of Perpignan).

3 Method, accuracy, repeatability, and quality control

3.1 Method and accuracy

Since 2003, the discrete samples returned back to SNAPO-CO_2 service facilities (LOCEAN, Paris) have been analyzed simultaneously for A_T and C_T by potentiometric titration using a closed cell (Edmond, 1970; Goyet et al., 1991). The same technique was used at sea for surface water underway measurements during OISO and MINERVE cruises (indicated by an asterisk in Table 1). In the late 1980s the JGOFS–IOC Advisory Panel on Ocean CO_2 recommended the need for standard analysis protocols and for developing certified reference materials (CRMs) for inorganic carbon measurements (Poisson et al., 1990; UNESCO, 1990, 1991). The CRMs were provided to international laboratories by Andrew Dickson (Scripps Institution of Oceanography, San Diego, USA), starting in 1990 for C_T and 1996 for A_T, respectively. These CRMs were thus always available to us and used to calibrate the measurements (CRM batch numbers used for each cruise are listed in the Supplement, Table S2). The CRM accuracy, as indicated in the certificate for each batch, is around $\pm 0.5\,\mu mol\,kg^{-1}$ for both A_T and C_T (https://www.nodc.noaa.gov/ocads/oceans/Dickson_CRM/batches.html, last access: 22 January 2025). The concentrations of CRMs we used vary between 2193 and $2426\,\mu mol\,kg^{-1}$ for A_T and between 1968 and $2115\,\mu mol\,kg^{-1}$ for C_T, corresponding to the range of concentrations observed in open-ocean water. In the Mediterranean Sea the concentrations are higher ($A_T > 2600\,\mu mol\,kg^{-1}$ and $C_T > 2300\,\mu mol\,kg^{-1}$), and in the coastal zones or near the Amazon River plume the concentrations were often lower than the CRMs ($A_T < 1500\,\mu mol\,kg^{-1}$ and $C_T < 1000\,\mu mol\,kg^{-1}$). Results of analyses performed on 1242 CRM bottles (different batches) in 2013–2024 are presented in Fig. 2. The standard deviations (SDs) of the differences in measurements were on average $\pm 2.69\,\mu mol\,kg^{-1}$ for A_T and $\pm 2.88\,\mu mol\,kg^{-1}$ for C_T. For unknown reasons, the differences were occasionally up to 10–15 $\mu mol\,kg^{-1}$ (1.2 % of the data; Fig. S2). These few CRM measurements were discarded for data processing. We did not detect any specific signal for CRM analyses (e.g., larger uncertainty depending on the batch number or temporal drifts during analyses; Fig. 2), but for some cruises the accuracy based on CRMs could be better than $3\,\mu mol\,kg^{-1}$ (e.g., $< 3\,\mu mol\,kg^{-1}$ for AMAZOMIX cruise using six batches of no. 197 and for MOOSE-GE 2022 using 19 batches of no. 204, or $< 1.5\,\mu mol\,kg^{-1}$ for SOMLIT-Point-B in 2022 using six batches of no. 204).

3.2 Repeatability

For some projects, duplicates have been regularly sampled (SOMLIT-Point-B, SOMLIT-Brest) or replicate bottles sampled at selected depths at fixed stations during the cruises (e.g., STEP, CARBODISS). In the first synthesis of the SNAPO-CO_2 dataset, we showed the results from several time series (SOMLIT-Point-B, SOMLIT-Brest and BOUSSOLE/DYFAMED). Here we present the results for the new data obtained at SOMLIT-Point-B in the coastal Mediterranean Sea and SOMLIT-Brest in the Bay of Brest (Fig. 3). Results of A_T and C_T repeatability are synthesized in Table 2. For the OISO cruises conducted in 2019, 2020, and 2021, the repeatability was evaluated from duplicate analyses (within 20 min) of continuous sea surface underway sampling at the same location (when the ship was stopped). Similarly to what was found for the CRM measurements (Fig. S2), differences in duplicates are occasionally higher than 10–15 $\mu mol\,kg^{-1}$ (Fig. 3), but most of the duplicates for all projects are within 0 to $3\,\mu mol\,kg^{-1}$. Compared to previous results (Kapsenberg et al., 2017; Metzl et al., 2024a), there are larger differences between duplicates at SOMLIT-B in 2019–2023 (up to $30\,\mu mol\,kg^{-1}$; Fig. 3), leading to relatively large SDs around 5 and $6\,\mu mol\,kg^{-1}$ for both A_T and C_T (Table 2). The same was observed for duplicates at SOMLIT-Brest (Table 2). We do not yet have a clear explanation for this large SD, although larger variability was observed in recent years, and the measurements were performed later after the sampling (e.g., more than 6 months for some samples during and after the COVID period). We will see that, given the temporal variability in the properties, this does not lead to suspicious interpretation for the seasonality or the trend analyses of these time series.

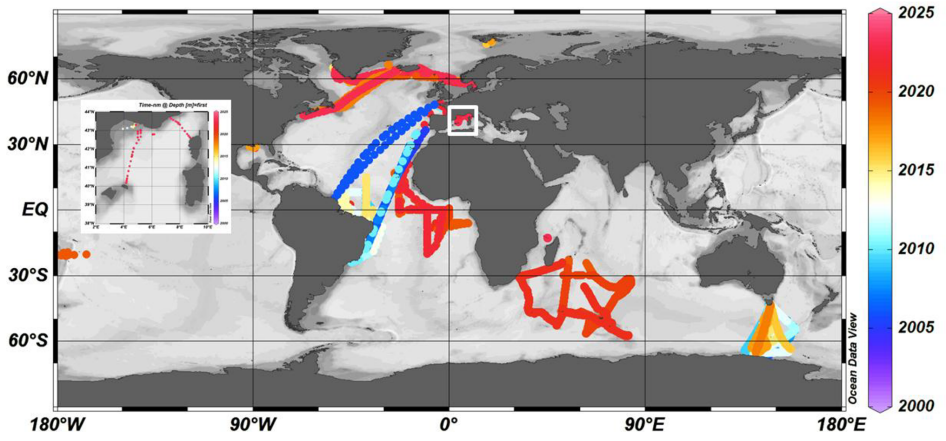

Figure 1. Locations of new A_T and C_T data (2005–2023) in the global ocean and the western Mediterranean Sea (white box, inset) in the SNAPO-CO_2-v2 dataset. Color code is for year. Figure produced with ODV (Schlitzer, 2018).

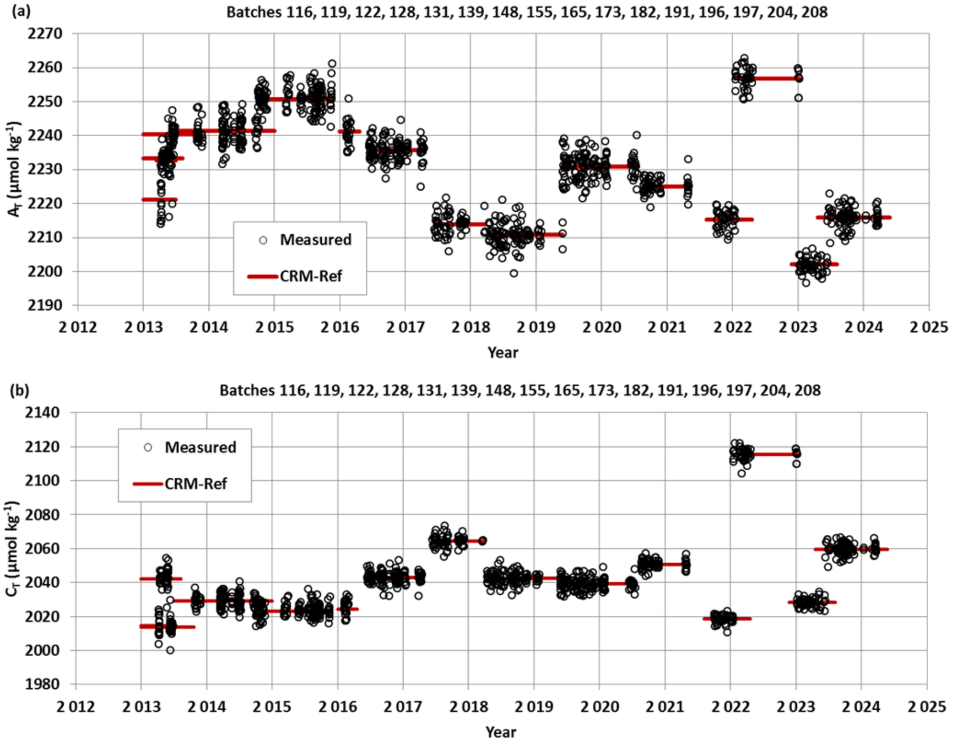

Figure 2. A_T **(a)** and C_T **(b)** analyses for different CRM batches measured in 2013–2024. For these 1242 analyses, the mean and standard deviations of the differences with the CRM reference were −0.11 (±2.69) µmol kg^{-1} for A_T and 0.01 (±2.88) µmol kg^{-1} for C_T.

3.3 Assigned flags for quality control

Identifying all data with an appropriate flag is very convenient for selecting the data (good, questionable, or bad). Here we used four flags for each property (flag 2 for good, 3 for questionable, 4 for bad, and 9 for no data) following the WOCE program and those used in other data products such as SOCAT (Bakker et al., 2016) and GLODAP (Olsen et al., 2016; Lauvset et al., 2024). During the data processing, we first assigned a flag for all A_T and C_T data based on the standard error in the calculation of A_T and C_T concentrations (nonlinear regression; Dickson et al. 2007). By default, if the standard deviation on the regression is > 1 µmol kg^{-1}, we assigned flag 3 (questionable), although the data could be acceptable and then used for interpretations. Flag 3 was also assigned when salinity was doubtful or when differences in duplicates were large (e.g., ±20 µmol kg^{-1}). Flag 4 (bad or certainly bad) was assigned when clear anomalies were detected for unknown reasons (e.g., a sample probably not fixed

Table 1. List of cruises added to the SNAPO-CO_2-v2 dataset. This is organized by region from north to south and the Mediterranean Sea (MedSea). See Tables S1, S2, S3, and S4 in the Supplement for a list of laboratories, CRMs used, DOIs, and references of cruises. No. denotes the number of data for each cruise or time series. An asterisk indicates the measurements at sea (surface underway).

Cruise/project	Start	End	Region	Sampling	No.
STEP	2016	2017	Arctic	Water column	33
SURATLANT AX1	2017	2023	North Atlantic	Surface	255
SURATLANT AX2	2018	2023	North Atlantic	Surface	224
VOS	2005	2010	Atlantic	Surface	192
MISSRHODIA-1	2017	2017	Gulf of Mexico	Water column	8
ACIDHYPO	2022	2022	Gulf of Mexico	Water column	10
CAMFIN-WATL	2010	2015	Tropical Atlantic	Surface	192
PIRATA-BR	2009	2015	Tropical Atlantic	Surface	194
BIOAMAZON	2013	2014	Tropical Atlantic	Surface	62
AMAZOMIX	2021	2021	Tropical Atlantic	Water column	180
PIRATA-FR	2019	2019	Tropical Atlantic	Surface	93
PIRATA-FR	2020	2020	Tropical Atlantic	Surface, water column	58
PIRATA-FR	2021	2021	Tropical Atlantic	Surface, water column	79
PIRATA-FR	2022	2022	Tropical Atlantic	Surface, water column	118
CO_2ARVOR	2009	2010	Atlantic, coastal	Surface, water column	621
SOMLIT-Roscoff	2020	2022	Coastal North Atlantic	Surface and 60 m	207
SOMLIT-Brest	2020	2022	Coastal North Atlantic	Surface	251
TONGA	2019	2019	Tropical Pacific	Water column	226
CARBODISS	2018	2019	Indian Ocean, Mayotte	Surface	85
OISO*	2019	2021	South Indian	Surface	5258
MINERVE	2004	2018	Southern Ocean	Surface	1077
MINERVE*	2002	2013	Southern Ocean	Surface	11 258
COCORICO$_2$	2017	2022	Coastal	Surface	589
SOMLIT-Point-B	2019	2023	MedSea coastal	Surface and 50 m	716
SOLEMIO	2018	2022	MedSea coastal	Water column	271
ANTARES	2017	2023	MedSea	Water column	506
MOLA	2018	2023	MedSea coastal	Water column	193
DYFAMED	2018	2023	MedSea	Water column	514
MESURHO-BENT	2010	2011	MedSea coastal	Surface and subsurface	25
ACCESS-01	2012	2012	MedSea coastal	Water column	16
CARBO-DELTA-2	2013	2013	MedSea coastal	Water column	14
DICASE	2014	2014	MedSea coastal	Water column	22
MISSRHODIA-2	2018	2018	MedSea coastal	Surface and subsurface	13
DELTARHONE1	2022	2022	MedSea coastal	Water column	9
MOOSE-GE	2021	2021	MedSea	Water column	451
MOOSE-GE	2022	2022	MedSea	Water column	447
MOOSE-GE	2023	2023	MedSea	Water column	475

with $HgCl_2$ or analysis performed late during COVID). A secondary quality control was performed by the PIs of each project based on data inspection, duplicates, the A_T–salinity relationship, or the mean observations in deep layers where large variability in A_T and C_T is unlikely to occur from year to year.

An example of quality flag is presented for all data from the MINERVE cruises conducted in 2002–2018 in the Southern Ocean, where clear outliers have been identified (Fig. S3). For the MINERVE cruises in 2002–2018 and a total of 12 335 A_T and C_T analyses, 24 were identified as bad (flag 4), 978 for A_T and 971 for C_T were listed as questionable (flag 3), and all others are considered good data (flag 2, i.e., about 92 %). For the MOOSE-GE cruises in 2021, 2022, and 2023 (new data in SNAPO-CO_2-v2) and a total of 1373 A_T and C_T analyses, 2 were identified as bad (flag 4), 38 for A_T and 33 for C_T were listed as questionable (flag 3), and all others were considered good data (flag 2, i.e., 97 %). This is better than the statistics we evaluated for the SNAPO-CO_2-v1 dataset (90 % flag 2 for MOOSE-GE in 2010–2019). A similar control was performed for each project.

3.4 Intercomparisons

Intercomparisons of measurements performed for different cruises or with different techniques help to evaluate the qual-

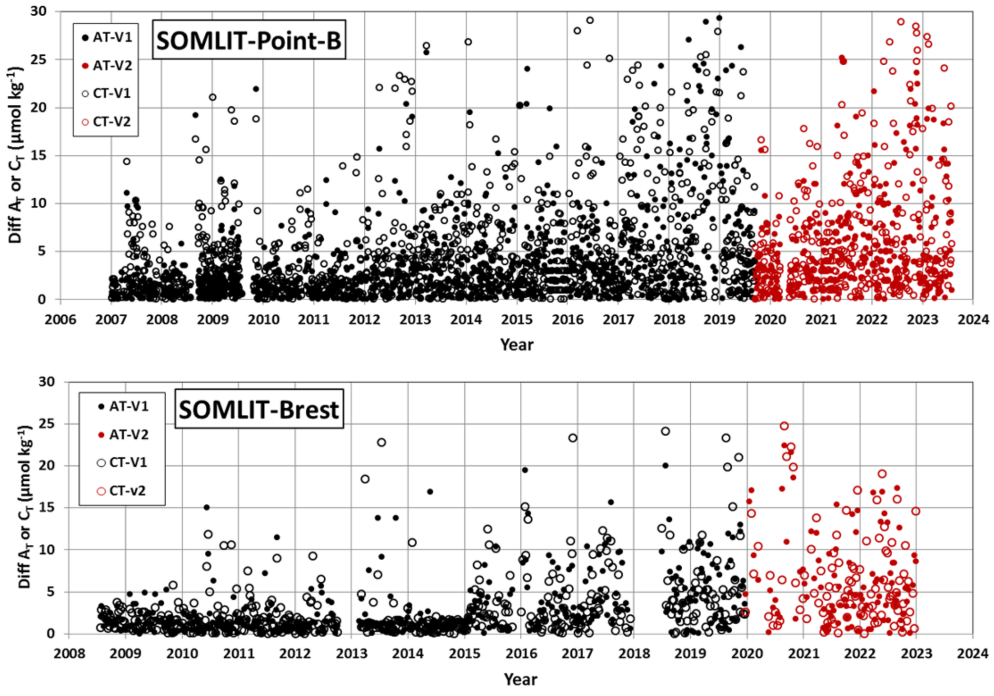

Figure 3. Results of duplicate A_T and C_T analyses from the time series SOMLIT-Point-B in the coastal Mediterranean Sea and SOMLIT-Brest off the coast of Brittany for the data in the SNAPO-CO_2-v1 dataset (black) and new data added to SNAPO-CO_2-v2 (red). The plots show differences in duplicates for both A_T (filled circles) and C_T (open circles). Standard deviations of these duplicates are listed in Table 2.

Table 2. Repeatability of A_T and C_T analyses for cruises with duplicate analysis. The results are expressed as the standard deviations (SDs) of the analysis of replicated samples. No. denotes the number of replicates for each time series or cruise. For the OISO cruises, the mean repeatability was obtained from measurements at the same location (when the ship stopped).

Cruise	Period	No.	SD A_T µmol kg^{-1}	SD C_T µmol kg^{-1}	Reference
STEP	2017	3	0.7	2.8	Unpublished
CARBODISS	2018	10	6.72	5.71	Unpublished
SOMLIT-Point-B	2007–2019	1130	4.5	5.1	SNAPO-CO_2-v1[a]
SOMLIT-Point-B	2019–2023	321	5.2	6.2	SNAPO-CO_2-v2[a]
SOMLIT-Brest	2008–2018	404	3.1	3.4	SNAPO-CO_2-v1[a]
SOMLIT-Brest	2019–2022	142	6.0	6.1	SNAPO-CO_2-v2[a]
OISO 29	2019	46	1.8	1.8	Leseurre et al. (2022)[b]
OISO 30	2020	67	1.5	2.0	Metzl et al. (2022)[b]
OISO 31	2021	343	2.6	3.3	Metzl et al. (2025)[b]

[a] See Fig. 3 for the results of regular duplicates for time series SOMLIT-Point-B and SOMLIT-Brest. [b] Metadata and data are available at https://www.nodc.noaa.gov/ocads/oceans/VOS_Program/OISO.html (last access: 22 January 2025).

ity of the data and detect potential biases when merging the data in the same region obtained by different laboratories at different periods. This is especially important to interpret long-term trends in A_T and C_T as well as for pCO_2 and pH calculated with A_T–C_T pairs. The synthesis of various cruises in the same region and periods also offers verification and secondary control of the data.

3.4.1 Comparisons in deep layers

Comparisons of data in the deep layers from different cruises are useful for secondary quality control as one expects low natural variability or anthropogenic signals from season to season and over a few years. Several cruises were conducted in the Mediterranean Sea in 2017–2023 (MOOSE-GE, ANTARES and DYFAMED). The mean values of C_T and A_T in the deep layers (> 1800 m) for each cruise confirmed the coherence of the data (Table 3). The C_T and A_T

concentrations are also in the range of the mean values evaluated for cruises conducted in 2014 in the Mediterranean Sea (results listed in the SNAPO-CO_2-v1 synthesis; Metzl et al., 2024a). In the western tropical Pacific we also observed coherent properties for the TONGA and OUTPACE cruises (Wagener et al., 2018) for data selected at 1800–2300 m layer, corresponding to the C_T maximum layer in the Pacific Deep Water (PDW). On the other hand in the western tropical Atlantic near the Amazon River plume, where the spatial variability in the properties is large at the surface (Ternon et al., 2000; Mu et al., 2021; Olivier et al., 2022), the comparison in the water column is less clear (Fig. S4). Nevertheless for the AMAZOMIX and the TARA-Microbiome cruises, both conducted in September 2021, the results at close stations (around 5° N, 50° W) suggest very similar concentrations at 1000 m (Table 3). The comparisons in deep waters enabled us to merge the different datasets for interpretation of the temporal trends and processes driving the CO_2 cycle in these regions (e.g., Ulses et al., 2023, and Wimart-Rousseau et al., 2023, for the Mediterranean Sea).

3.4.2 Comparing onboard and onshore results

In surface waters where the variability is high, intercomparison is not relevant for secondary quality control. However, during the MINERVE cruises, discrete samples were occasionally performed along with sea surface underway measurements. Thus, we can compare A_T and C_T measured in the laboratory with those measured on board as described by Laika et al. (2009) for the MINERVE cruises in 2005–2006. It should be noticed that the discrete samples were measured after a long trip (shipping boxes from Hobart, Tasmania, to Paris, France) and thus generally analyzed at least 3 months after the cruises (cruises conducted in October to February, analyses performed in May–June). Given all the uncertainties associated with the sampling, sample storage and transport, analyses and CRMs, the mean differences between discrete and underway data are still reasonable (SDs ranging between 4 and 12 µmol kg^{-1}; Table 4). For unknown reasons the mean difference was high for a cruise in 2008–2009 (SD > 10 µmol kg^{-1}, the "weather goal"; Newton et al., 2015). With this in mind, we believe the MINERVE data (both underway and discrete data) are useful to interpret the change in properties in this region at seasonal or decadal scales (Laika et al., 2009; Brandon et al., 2022).

3.4.3 Comparison based on different techniques

Another example of comparison is presented for samples obtained in the lagoon of the island of Mayotte in the western Indian Ocean and measured using different techniques. In the framework of the CARBODISS project, seawater was sampled in 2018–2023 at several coral reef sites within the northeastern part of the lagoon and measured either at the LOCEAN laboratory or at Réunion University. To remove coral sand particles, the water samples were immediately filtered through Whatman GF/F filters and poisoned with mercuric chloride, following Dickson et al. (2007). In 2021, 2022, and 2023, A_T was measured at Réunion University using an automated potentiometric titration (905 Titrando Metrohm titrator with combined pH electrode 6.0253.00) and calculated from the second inflection point of the titration curve. The HCl concentration was checked each day of measurements using a CRM provided by Andrew Dickson, Scripps Institution of Oceanography. The A_T precision of ±2 µmol kg^{-1} was based on triplicate analyses (Lagoutte et al., 2023). In the studied coral reef sites, A_T concentrations ranged between 2250 and 2350 µmol kg^{-1} but with occasionally higher concentrations up to 2450–2500 µmol kg^{-1}. Such high A_T has been observed in other coral reef ecosystems (Cyronak et al., 2013, at the Cook Islands; Palacio-Castro et al., 2023, at Middle Keys, Florida). The data obtained in the lagoon of Mayotte on different coral reefs could be compared with underway observations obtained offshore of Mayotte (OISO-11 cruises in 2004 and CLIM-EPARSES cruise in 2019; data available in the SNAPO-CO_2-v1 dataset). In the open ocean the A_T concentrations ranged between 2250 and 2330 µmol kg^{-1}, close to the results obtained at Mayotte reefs except for samples in November 2021 that were all collected at Cratère station (12.84° S, 45.39° E) (Fig. 4). At this location there was a large diurnal variation in November 2021 with A_T increasing from 2322 to 2508 µmol kg^{-1} (Fig. S5). This is because in 2021 the samples were taken at low tide, allowing for the first time recording of the volcanic signal in this location (CO_2 resurgences). In 2018 and 2019 such high A_T values were not measured (Fig. S5) as samples were taken at high tides, allowing a certain dilution of volcanic CO_2 emissions in the water column. Although the samples were measured with different techniques, the range of A_T is coherent for both datasets (Fig. 4). Therefore, we added the A_T data measured at Réunion University in 2021–2023 to complete the synthesis for this location (Mayotte).

3.4.4 Summary of quality control data

The total number of data in the SNAPO-CO_2-v2 dataset for the global ocean is gathered in Table 5 with corresponding flags for each property. Overall, the synthesis includes more than 91 % of good data for both A_T and C_T. About 6 % are questionable, and 3 % are likely bad. Overall, we believe that all data (with flag 2) in this synthesis have an accuracy better than 4 µmol kg^{-1} for both A_T and C_T, the same as for quality-controlled data in GLODAP (Lauvset et al., 2024). The uncertainty ranges between the "climate goal" (2 µmol kg^{-1}) and the "weather goal" (10 µmol kg^{-1}) for ocean acidification studies (Newton et al., 2015; Tilbrook et al., 2019). This accuracy is also relevant to validate or constrain data-based methods that reconstruct A_T and C_T fields with an error of around 10–15 µmol kg^{-1} for both properties

Table 3. Mean observations in the deep layers (> 1800 m) of the Ligurian Sea (western Mediterranean Sea for different cruises conducted in 2017–2023), of the tropical Pacific (around 2000 m for cruises in 2017 and 2019), and of the tropical Atlantic (around 1000 m for cruises in 2021). N-A_T and N-C_T are A_T and C_T normalized at salinity ($S = 38$ in the Ligurian Sea; $S = 35$ for the Pacific and the Atlantic oceans). No. denotes the number of data (with flag 2). Standard deviations are in brackets.

Cruise	Period	No.	Potential temperature °C	Salinity	N-A_T µmol kg^{-1}	N-C_T µmol kg^{-1}
Ligurian Sea (> 1800 m)						
All cruises	2017–2023	227	12.923 (0.052)	38.484 (0.003)	2558.3 (10.5)	2300.0 (10.7)
DYFAMED	2017–2022	74	12.913 (0.006)	38.485 (0.002)	2555.1 (11.8)	2297.3 (12.4)
ANTARES	2017–2023	62	12.944 (0.096)	38.485 (0.005)	2559.8 (9.0)	2302.2 (8.9)
MOOSE-GE	2017–2023	91	12.917 (0.005)	38.484 (0.003)	2559.8 (9.8)	2300.7 (10.0)
Tropical Pacific (layer 1800–2300 m)						
OUTPACE	2017	15	2.124 (0.055)	34.633 (0.006)	2414.1 (8.0)	2318.8 (5.8)
TONGA	2019	7	2.196 (0.197)	34.619 (0.016)	2408.9 (9.1)	2327.2 (7.5)
Western tropical Atlantic (1000 m)						
AMAZOMIX	2021	14	4.770 (0.105)	34.711 (0.041)	2315.6 (20.2)	2220.8 (17.1)
TARA-MICRO	2021	1	4.852	34.717	2312.9	2231.1

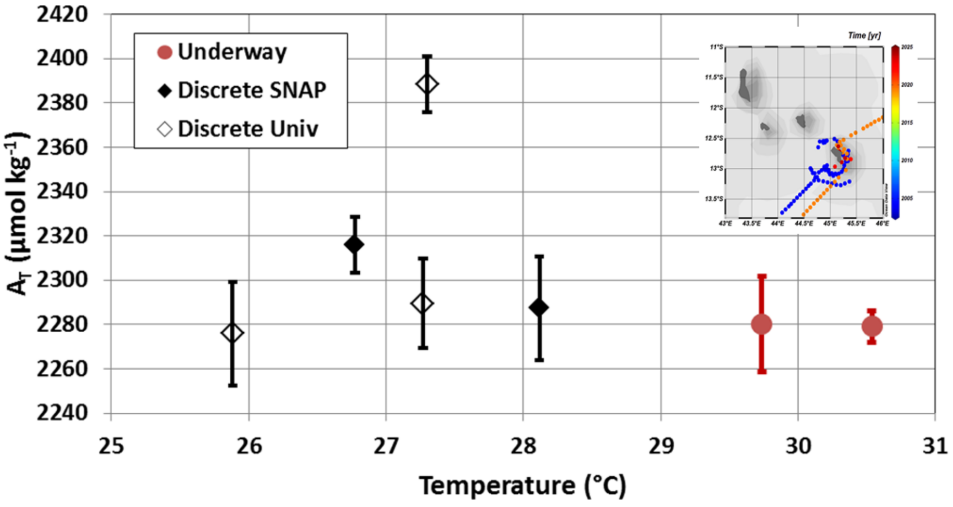

Figure 4. Total alkalinity (A_T) versus temperature for samples measured around Mayotte and in the coral reef (inset map). Underway A_T was measured on board in 2004 and 2019 (red circles), whereas discrete samples at different reef sites within the lagoon of Mayotte in 2018, 2019, 2021, 2022, and 2023 were measured at LOCEAN (black diamonds) or at Réunion University (open diamonds). The figure presents the data averaged for each cruise in this region.

Table 4. Comparison of A_T and C_T analyzed on board and at SNAPO-CO_2 facilities for the MINERVE project. The results are expressed as the standard deviations (SDs) of the differences for each cruise. No. denotes the number of co-located samples.

Period	No.	SD A_T µmol kg^{-1}	SD C_T µmol kg^{-1}
2004–2005	109	12.85	4.99
2005–2006	45	4.20	6.77
2007–2008	17	10.15	10.62
2008–2009	26	15.80	12.02
2009–2010	22	4.04	5.78
2010–2011	33	9.36	6.83
2012–2013	29	5.43	9.73

Table 5. Number of temperature, salinity, A_T, and C_T data in the SNAPO-CO_2-v2 synthesis identified for flags 2 (good), 3 (questionable), 4 (bad), and 9 (no data). The last column is the percentage of flag 2 (good).

Property	Flag 2	Flag 3	Flag 4	Flag 9	% flag 2
Temperature	68 253	418	0	653	99.4
Salinity	68 706	482	5	131	99.3
A_T	61 249	3910	2077	2088	91.1
C_T	61 869	3865	2057	1533	91.3

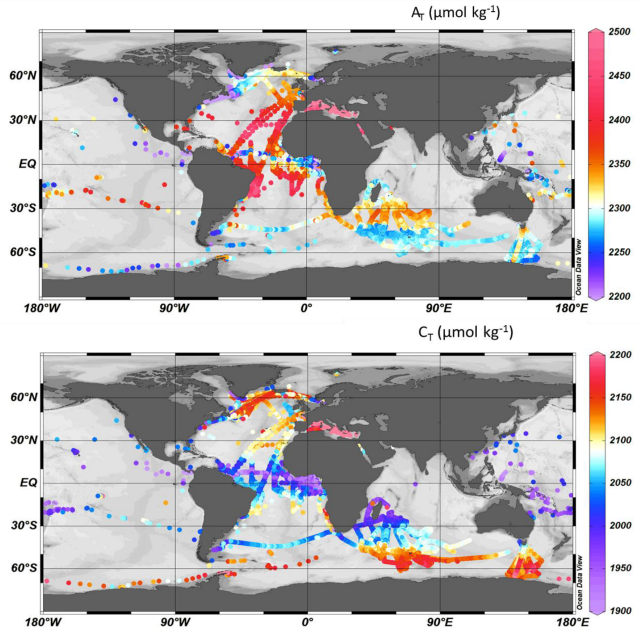

Figure 5. Distribution of A_T (top) and C_T (bottom) concentrations (µmol kg^{-1}) in surface waters (0–10 m) in the SNAPO-CO_2-v2 dataset. Only data with flag 2 are presented in these figures. Figures produced with ODV (Schlitzer, 2018).

(Bittig et al., 2018; Broullón et al., 2019, 2020; Fourrier et al., 2020; Gregor and Gruber, 2021; Chau et al., 2024a).

4 Global A_T and C_T distribution based on the SNAPO-CO_2-v2 dataset

The surface distribution in the global ocean based on the SNAPO-CO_2 dataset is presented in Fig. 5 for A_T and C_T. The A_T–salinity and A_T–C_T relationships are clearly identified and structured at regional scale (Fig. 6). In the open ocean, high A_T concentrations (> 2400 µmol kg^{-1}) are identified in the Atlantic subtropics (bands 35–15° N and 25–3° S) (Jiang et al., 2014; Takahashi et al., 2014). The lowest A_T and C_T concentrations (< 600 µmol kg^{-1}) are observed in the western tropical Atlantic in the Amazon River plume near the mouth (Lefèvre et al., 2017). For C_T the concentrations are high (> 2150 µmol kg^{-1}) in the Southern Ocean south of the polar front, associated with the deep mixing in winter and the upwelling of deep water (Metzl et al., 2006; Pardo et al., 2017). The highest C_T concentrations (up to 2180–2270 µmol kg^{-1}) are observed in the high latitudes of the Southern Ocean near the Adélie coastal zone (MINERVE and ACE cruises), around the Kerguelen Plateau (OISO-31 cruise) and close to the Antarctic Peninsula (TARA-Microbiome cruise). In the North Atlantic the new data from SURATLANT cruises in 2018–2023 confirm the high C_T concentrations (> 2150 µmol kg^{-1}) observed in the subpolar gyre since 2016 due in part to the accumulation of anthropogenic CO_2 (Leseurre et al., 2020). Low C_T concentrations (< 2000 µmol kg^{-1}) are found in the tropics (10° N–30° S) with lower values (< 1950 µmol kg^{-1}) in the equatorial Atlantic band 10° N to the Equator (e.g., Koffi et al., 2010; Lefèvre et al., 2021). In the Amazon shelf sector C_T can reach even lower concentrations (< 1700 µmol kg^{-1}, AMAZOMIX cruise).

5 Regional A_T and C_T distributions and trends based on the SNAPO-CO_2 dataset

The regional distributions are described for the Mediterranean Sea and for selected regions in the open ocean and coastal zones, where the data are available for 10 years or more to explore the A_T and C_T trends. Given the observed seasonal and interannual variability and the fact that the time series were not regular (e.g., at monthly frequency), we cannot use recommended methods to estimate the trends (e.g., based on deseasoned data; Sutton et al., 2022). Here we have selected the locations and seasons where the C_T trends can be linearly fitted and compared with no interpolation to fill gaps and discontinuous data (e.g., fewer samples during COVID).

5.1 The Mediterranean Sea

Compared to the open ocean, A_T concentrations are much higher in the Mediterranean Sea (Copin-Montégut, 1993;

Schneider et al., 2007; Álvarez et al., 2023) with values up to 2600 µmol kg^{-1}. The A_T and C_T data obtained in 2014–2023 show a clear contrast between the northern and southern regions of the western Mediterranean Sea with higher concentrations in the Ligurian Sea and the Gulf of Lion (Fig. 7). This contrast is associated with the circulation and the frontal system in this region (e.g., Barral et al., 2021). New data in the coastal zones in the Gulf of Lion (ACCESS, DICASE, CARBODELTA, COCORICO$_2$, MESURHOBENT) also have very high A_T and C_T concentrations ($A_T > 2600$ µmol kg^{-1}; $C_T > 2350$ µmol kg^{-1}). Very low A_T and C_T concentrations ($A_T < 2500$ µmol kg^{-1}; $C_T < 2200$ µmol kg^{-1}) were also occasionally observed in the coastal zones (COCORICO$_2$ stations; Petton et al., 2024).

In summer 2022 the Mediterranean Sea experienced an exceptional warming (Fig. S6) superposed to the long-term warming in the ocean (Cheng et al., 2024). Such an event would impact the internal ocean processes such as thermodynamic, stratification, and biological processes (Coppola et al., 2023) and the interannual variability and trends in C_T, pH, fCO_2, and air–sea CO_2 fluxes (Yao et al., 2016; Wimart-Rousseau et al., 2023; Chau et al., 2024b). As in 2003, the warming in summer 2022 was associated with the drought event that occurred in Europe and over the Mediterranean Sea (Faranda et al., 2023). In July 2022, the maximum temperature of 28.42 °C was observed at station SOMLIT-Point-B. In the Ligurian Sea the temperature trend has been faster in recent years: $+0.173 \pm 0.072$ °C per decade over 1990–2010 and $+0.678 \pm 0.143$ per decade over 2010–2023 (Fig. S6). With the new data added to the SNAPO-CO_2-v2 synthesis (DYFAMED, MOOSE-ANTARES, and MOOSE-GE), we evaluated a temperature trend of $+0.84 \pm 0.20$ °C per decade over 1998–2022, indicating that the discrete sampling captured the property changes at regional scale. Based on the data in the Ligurian Sea, the trends in C_T appeared faster in summer ($+1.53 \pm 0.46$ µmol kg^{-1} yr^{-1}) than in winter ($+0.94 \pm 0.64$ µmol kg^{-1} yr^{-1}; Table 6). On the other hand, the trends in A_T were the same ($+0.72 \pm 0.36$ µmol kg^{-1} yr^{-1} in winter and $+0.69 \pm 0.42$ µmol kg^{-1} yr^{-1} in summer). The trend in C_T on the surface in winter was close to the one derived at 100 m (below the Chl *a* maximum), $C_T^{100\,m} = +1.10 \pm 0.17$ µmol kg^{-1} yr^{-1} (Fig. 8), whereas for A_T the trend was the same at the surface and at depth ($+0.76 \pm 0.12$ µmol kg^{-1} yr^{-1}). This suggests that the winter C_T data recorded the anthropogenic CO_2 uptake of around $+1$ µmol kg^{-1} yr^{-1}; Fig. S7). Note that, given the observed C_T trends, the spatial view presented in Fig. 7b for 2014–2023 would be the same based on C_T concentrations normalized to a reference year. As noted by Touratier and Goyet (2009), the C_T concentrations in the Mediterranean Sea should increase in parallel with the level of atmospheric anthropogenic CO_2. For an atmospheric CO_2 rate of $+2.16$ ppm yr^{-1} over 1998–2023 (Lan et al., 2024) and at fixed sea surface temperature (17.75 °C), salinity (38.25), and A_T (2567 µmol kg^{-1}), the theoretical C_T increase would be $+1.24$ µmol kg^{-1} yr^{-1}. Interestingly, an anthropogenic flux of -0.3 ± 0.02 molC m^{-2} yr^{-1} in the Mediterranean Sea (Bourgeois et al., 2016) would correspond to an increase in C_T of 1.07 ± 0.07 µmol kg^{-1} yr^{-1} in the top 100 m. This is again close to what is observed in winter or at 100 m (Table 6, Fig. 8). On the other hand the faster C_T trend observed in surface waters during summer might be associated with a decrease in biological production and/or changes in circulation/mixing over time that deserve specific investigations, such as an analysis of the oxygen budget in this region (Ulses et al., 2021). It is worth noting that the C_T and A_T trends in coastal zones of the Mediterranean Sea are the opposite of those observed offshore: for example at station SOLEMIO (Bay of Marseille; Wimart-Rousseau et al., 2020), the C_T and A_T concentrations decreased over 2016–2022 and thus opposed the anthropogenic CO_2 signal, indicating that processes such as riverine inputs, advection, and biology control the carbonate system decadal variability at local scale. This calls for developing dedicated complex biogeochemical models to resolve these processes (Barré et al., 2023, 2024), especially when extreme events occur, such as the very hot summer in 2024 with sea surface temperature (SST) up to 30 °C in the Mediterranean Sea (platform buoy and/or mooring AZUR, EOL, and La Revellata, data available at https://dataselection.coriolis.eu.org/, last access: 11 October 2024). The data obtained in the Mediterranean Sea are important not only to validate biogeochemical models but also to reconstruct the carbonate system from A_T and pCO_2 data (Chau et al., 2024a) as the global A_T–sea surface salinity (SSS) relationships (e.g., Carter et al., 2018) are not suitable for this region.

5.2 The North Atlantic

The North Atlantic Ocean is an important CO_2 sink (Takahashi et al., 2009) due to biological activity during summer and heat loss and deep convection during winter. As a result this region contains high concentrations of anthropogenic CO_2 (C_{ant}) in the water column (Khatiwala et al., 2013). Decadal variations in the C_{ant} inventories were recently identified at basin scale, probably linked to the change in the overturning circulation (Gruber et al., 2019; Müller et al., 2023; Pérez et al., 2024). This region experienced climate modes such as the North Atlantic Oscillation (NAO) and the Atlantic Multidecadal Variability (AMV) that imprint variability in air–sea CO_2 fluxes at interannual to multidecadal scales (e.g., Thomas et al., 2008; Jing et al., 2019; Landschützer et al., 2019) but not always clearly revealed at regional scale (Metzl et al., 2010; Schuster et al., 2013; Pérez et al., 2024). In addition it has been recently shown that extreme events such as the marine heat wave in summer 2023 led to a reduce CO_2 uptake in this region (Chau et al., 2024b). Although the annual CO_2 fluxes deduced from global ocean biogeochemical models (GOBMs) seem coherent with the data products

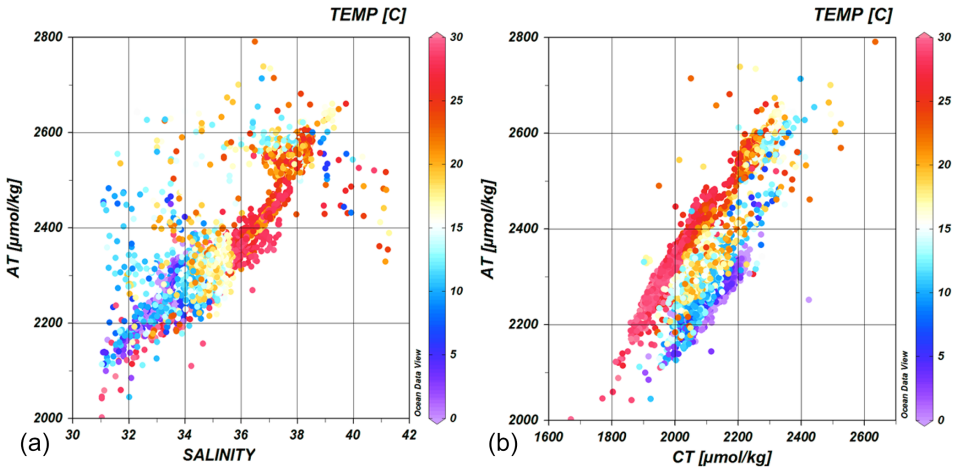

Figure 6. Relationships between A_T and salinity **(a)** and A_T versus C_T **(b)** for samples in surface waters (0–10 m and salinity > 31). Only data with flag 2 are presented (no. = 48 749). The color scales correspond to the temperature. The data not aligned correspond to coastal zones (e.g., COCORICO$_2$ stations). Figures produced with ODV (Schlitzer, 2018).

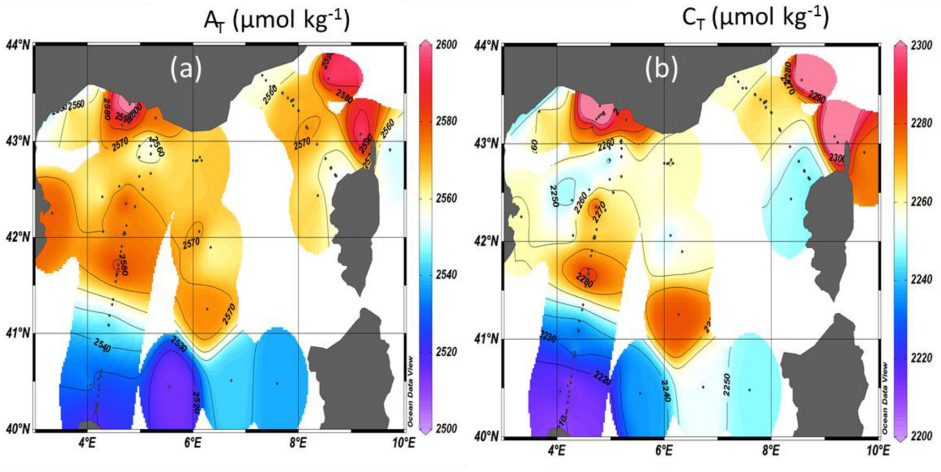

Figure 7. Distribution of A_T **(a)** and C_T **(b)** in µmol kg^{-1} in surface waters of the Mediterranean Sea (0–10 m) from observations over 2014–2023. Figures produced with ODV (Schlitzer, 2018).

at basin scale (-0.30 ± 0.07 and -0.24 ± 0.03 PgC yr^{-1} for the North Atlantic subpolar seasonally stratified, NA-SPSS biome), the pCO_2 cycle seasonality is not well simulated (Pérez et al., 2024). Therefore to correct the GOBMs outputs, comparisons with the observed C_T and A_T cycles are also needed.

In this context regular sampling in the North Atlantic (OVIDE cruises, Mercier et al., 2015, 2024; SURATLANT transects, Reverdin et al., 2018) and time-series stations in the Irminger and Iceland seas (Olafsson et al., 2010; Lange et al., 2024; Yoder et al., 2024) are important to explore the variability in the biogeochemical properties from seasonal (Fig. S8) to decadal scales (Fig. 9). The SURATLANT data added to the SNAPO-CO_2-v2 dataset over 2017–2023 offer new observations in the North Atlantic Subpolar Gyre (NASPG in the NA-SPSS biome) and new transects from Norway to Iceland and reaching the coast of Greenland (Fig. 9). In 2010 the winter NAO was negative, moved to a positive state in 2012–2020, and was again very low in 2021. The new SURATLANT data after 2017 confirm the cooling and the freshening in the NASPG since 2009 (Holliday et al., 2020; Leseurre et al., 2020; Siddiqui et al., 2024), whereas the most recent data in 2022 and 2023 suggest a reverse trend (increase in salinity and temperature; Fig. S8). After 2016, large C_T anomalies in the NASPG were observed. For example, in April 2019 and 2022, the C_T concentrations were low compared to 2016 (Fig. 9) and opposed to the expected anthropogenic CO_2 uptake. In September 2023 the C_T concentrations were much lower than in 2022 (Fig. 9), probably linked to biological productivity when the NAO index was negative (Fröb et al., 2019), as observed in summer 2023 (NAO < -2 in

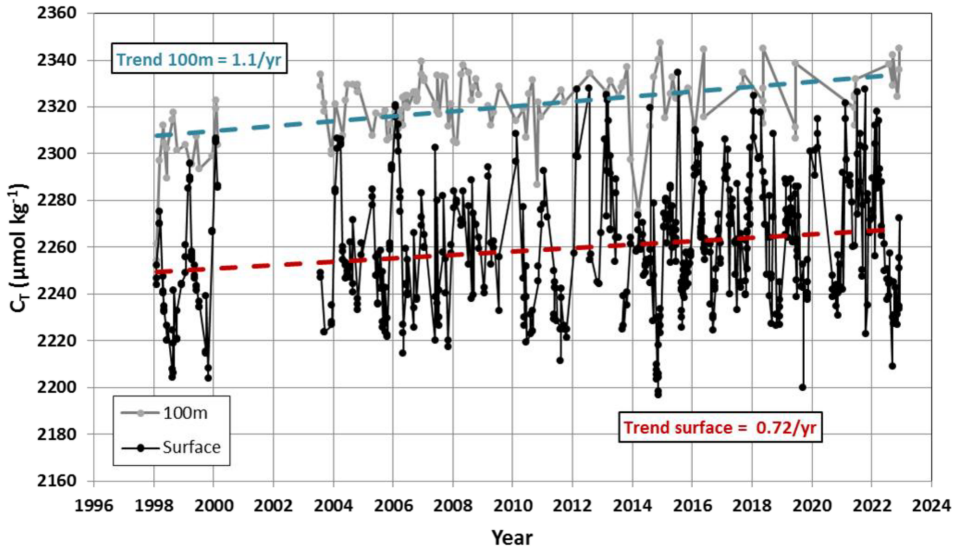

Figure 8. Time series of C_T concentrations at the surface (black symbols) and at 100 m (grey symbols) in the Ligurian Sea. The trends over 1998–2022 at the surface (red) and at 100 m (blue) are indicated by dashed lines.

Table 6. Trend in C_T (µmol kg^{-1} yr^{-1}) and corresponding standard error in selected regions where data are available for more than 10 years. The projects/cruises for the selection of the data in each domain are indicated.

Region	Period/season	C_T trend (µmol kg^{-1} yr^{-1})	Projects/cruises
North Atlantic (NASPG)	1994–2023 April	+0.78 (0.23)	SURATLANT
North Atlantic (NASPG)	1994–2023 September	+1.09 (0.37)	SURATLANT
Western tropical Atlantic 5° N to the Equator	2009–2021 April–October	+3.31 (2.13)	AMAZOMIX, PIRATA-BR, TARA
Western tropical Atlantic Equator to 10° S	2005–2015 April–October	+3.05 (1.64)	CAMFIN-WATL, PIRATA-BR, VOS
Ligurian Sea 8E	1998–2022 January–February	+0.94 (0.64)	ANTARES, DYFAMED, MOOSE-GE
Ligurian Sea 8E	1998–2023 July–August	+1.53 (0.46)	ANTARES, DYFAMED, MOOSE-GE
Subtropical Indian 37S	1998–2020 January–February	+1.12 (0.36)	OISO
Southwestern Indian 50S	1998–2021 January–February	+0.61 (0.21)	OISO
Southwestern Indian 56S	1998–2020 January–February	+0.58 (0.27)	OISO
Southwestern Indian 56S	2015–2020 January–February	+3.41 (0.73)	OISO
Southeastern Indian 60S	2002–2012 January–February	+3.37 (0.94)	MINERVE, OISO
Southeastern Indian 60S	2002–2012 October	+4.79 (1.62)	MINERVE

July 2023). Despite this variability the C_T trends are relatively well evaluated (Table 6). As in the Mediterranean Sea the C_T trends in the NASPG appeared to be different depending on the season (Fig. 9). The C_T increase was faster in September than in April ($+1.09 \pm 0.37$ µmol kg^{-1} yr^{-1} and $+0.78 \pm 0.23$ µmol kg^{-1} yr^{-1}). This is either close to or lower than the theoretical C_T increase due to the rise of atmospheric CO_2 ($+0.91$ µmol kg^{-1} yr^{-1}) and in the range of recent results evaluated for the subpolar mode waters in the Irminger Sea (C_{ant} trend $= 0.95 \pm 0.17$ µmol kg^{-1} yr^{-1} for the period 2009–2019; Curbelo-Hernández et al., 2024).

5.3 The tropical Atlantic

In the tropical Atlantic, previous studies highlighted the large variability of biogeochemistry and the difficulty in detecting long-term trends in C_T (e.g., Lefèvre et al., 2021). This is related to the variability of circulation, equatorial upwelling, biological processes (some linked to Saharan dust), and inputs from large rivers (Congo, Amazon, and Orinoco). The new data added to version SNAPO-CO_2-v2 (Fig. S9) show the contrasting zonal C_T distribution in this region with lower concentrations in low-salinity regions of the North Equatorial Counter Current and Guinea Current (Fig. 5; Oudot et al., 1995; Takahashi et al., 2014; Broullón et al., 2020; Bonou et al., 2022). For exploring the temporal changes, we selected

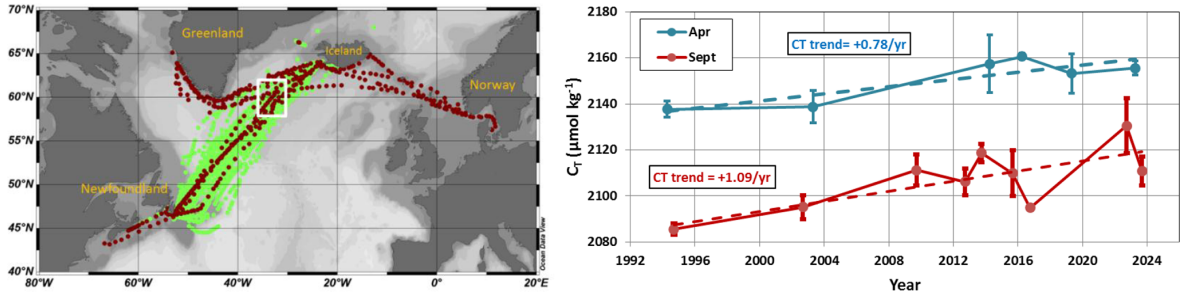

Figure 9. On the left are data from SNAPO-CO_2-v1 (green) and new data in v2 (brown) from the SURATLANT cruises in 1993–2023 in the North Atlantic. Figure produced with ODV (Schlitzer, 2018). The white box identifies the region of selected data around 60° N for the trend analysis. On the right are time series of average C_T concentrations in April (blue) and September (red) in this region. The trends for each season are indicated (see also Table 6).

the data in the western region, available for at least 10 years, and separated them into the northern and southern sectors. In both regions the C_T trend is close to $+3\,\mu mol\,kg^{-1}\,yr^{-1}$ (Table 6, Fig. S9), much higher than the excepted anthropogenic signal. In this region where coastal water masses mix with oceanic waters, the interannual variability in C_T is large and the changes driven by competitive processes (circulation, biological processes). More observations and dedicated models are needed to separate the anthropogenic and natural variability in this region (Pérez et al., 2024).

5.4 The Southern Ocean

In the Southern Ocean there are a few regular multiannual observations of the carbonate system. Time series of more than 10 years were obtained in the Drake Passage (Munro et al., 2015) and in the southern Indian Ocean (Leseurre et al., 2022; Metzl et al., 2024b). Observations were also obtained for more than 20 years southeast of New Zealand from the Munida Time Series (MTS) in the subtropical and sub-Antarctic frontal zones (Currie et al., 2011; Vance et al., 2024). To complement these datasets we have added the data collected in the southeastern Indian Ocean between Tasmania and Antarctica in the framework of the MINERVE cruises (Fig. 10; Brandon et al., 2022). These cruises were conducted from October to March, offering each year a view of the seasonal changes between late winter and summer from the sub-Antarctic zone to the coastal zone near Antarctica (Adélie Land). In all sectors (here from 45 to 67° S), the C_T concentrations were higher in October when the mixed-layer depth (MLD) was deep and were lower during the productive summer season (e.g., Laika et al., 2009; Shadwick et al., 2015). An example is presented at 60° S, 151° E from the data obtained along a reoccupied track in 2011–2012 (Fig. S10). At this location south of the polar front in the POOZ/HNLC area (permanent open ocean zone/high-nutrient low-chlorophyll area), the C_T concentrations were $+25\,\mu mol\,kg^{-1}$ higher in October compared to February. The same seasonal amplitude was observed in the western Indian sector of the POOZ (Metzl et al., 2006, 2024b), suggesting that the C_T seasonality is relatively homogeneous in this region, corresponding to the Indian SO–SPSS biome (Fay and McKinley, 2014). The difference in the climatological C_T between October and January is on average $+28.3 \pm 9.8\,\mu mol\,kg^{-1}$ in the Indian Ocean POOZ (Takahashi et al., 2014). Given this seasonality and potential change in the seasonal amplitude over time (Gallego et al., 2018; Landschützer et al., 2018; Shadwick et al., 2023), the property trends have to be evaluated for October and January–February separately, here over 2002–2012 in the POOZ (Fig. 10, Table 6). In both seasons, the average C_T concentrations reached a minimum in 2008 and increased faster in 2008–2012 (up to $+4.8\,\mu mol\,kg^{-1}\,yr^{-1}$). Interestingly, such an acceleration of the trend after 2009 was observed for pCO_2 at the MTS station (Vance et al., 2024). We note that the C_T trend over 2002–2012 was slightly faster in October (Fig. 10), probably linked to deeper MLD, as suggested from the cooling and the salinity increase observed during this season (Fig. S10).

In the western Indian sector, the new data in the SNAPO-CO_2-v2 dataset from the OISO cruises at high latitudes also recorded a rapid C_T trend over 5–8-year periods (e.g., $+3.4\,\mu mol\,kg^{-1}\,yr^{-1}$ in 2015–2020 at 56° S; Fig. 11, Table 6). Although the interannual variability in C_T, between 10 and $20\,\mu mol\,kg^{-1}$, is often recognized (Fig. 11), the evaluation of the trends over more than 20 years indicated a faster trend in the subtropical Indian Ocean ($+1.1\,\mu mol\,kg^{-1}\,yr^{-1}$) compared to higher latitudes (Indian POOZ, $+0.6\,\mu mol\,kg^{-1}\,yr^{-1}$); they are close to the expected anthropogenic signal in these regions ($+1.1\,\mu mol\,kg^{-1}\,yr^{-1}$ in the subtropics and $+0.8\,\mu mol\,kg^{-1}\,yr^{-1}$ at higher latitudes).

5.5 The coastal zones

Coastal waters experience enhanced ocean acidification due to increasing CO_2 uptake, due to accumulation of anthropogenic CO_2 (Bourgeois et al., 2016; Laruelle et al., 2018;

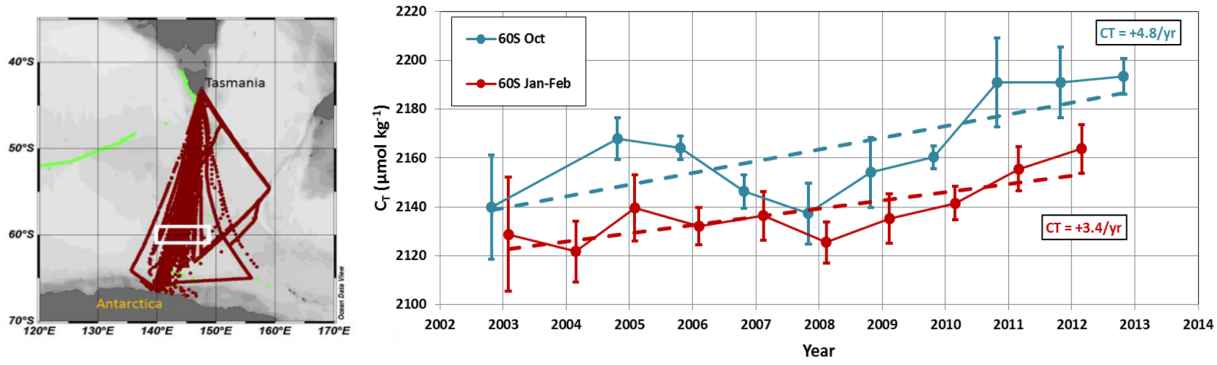

Figure 10. On the left are data from the SNAPO-CO_2-v1 dataset (green) and new data in version v2 (brown) in the southeastern Indian Ocean. Figure produced with ODV (Schlitzer, 2018). The white box identifies the region of selected data around 60° S for the trend analysis. On the right are time series of average C_T concentrations in January–February (red) and October (blue) around 60° S (white box in the map). The trends for each season are indicated (see also Table 6).

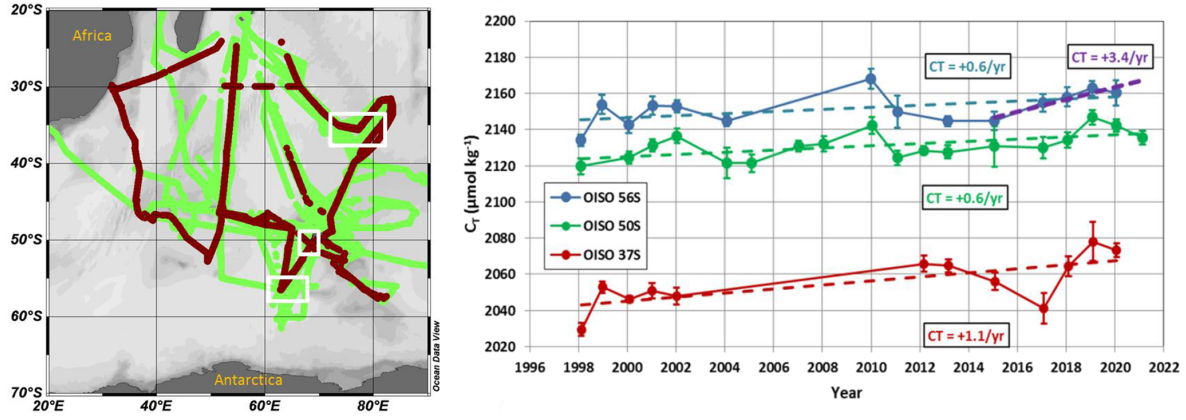

Figure 11. On the left are data from the SNAPO-CO_2-v1 dataset (green) and new data in version v2 (brown) in the southwestern Indian Ocean (OISO cruises). Figure produced with ODV (Schlitzer, 2018). The white boxes identify the regions of data selected around 37, 50, and 56° S for the trend analysis. On the right are time series of average C_T concentrations in January–February at 37° S (red), 50° S (green), and 56° S (blue). The trends for each region are indicated (see also Table 6).

Roobaert et al., 2024a; Li et al., 2024), and from local anthropogenic inputs through rivers or from air pollution (e.g., Sarma et al., 2015; Sridevi and Sarma, 2021; Wimart-Rousseau et al., 2020). The changes in the CO_2 uptake in coastal zones are also linked to biological processes (Mathis et al., 2024) or to circulation and local upwelling (Roobaert et al., 2024b), all controlling large variability in A_T and C_T in space and time, leading to uncertainties in detecting long-term changes in pCO_2 and air–sea CO_2 fluxes in heterogeneous coastal waters (Dai et al., 2022; Resplandy et al., 2024). At seasonal scale, large differences between observations and models were also identified, leading to differences in the coastal ocean CO_2 sink of up to 60 % (Resplandy et al., 2024). It is thus important to document the seasonal cycles of A_T and C_T to compare and correct models and thus to better predict future changes in biogeochemical properties in coastal waters and their impact on marine ecosystems. A better understanding of the processes and their retroaction in the coastal regions is also required regarding marine carbon dioxide removal (MCDR) experiments and for their evaluation (e.g., Ho et al., 2023).

In the SNAPO-CO_2-v2 dataset, new data have been added to the coastal zones at stations SOMLIT-Brest, SOMLIT-Roscoff, and SOMLIT-Point-B. They extend the period to 2022 or 2023 for temporal analysis. New data from the French coastal zones have been also included from the COCORICO$_2$ project documented in detail by Petton et al. (2024). The observations in coastal zones could be identified in the MARCATS regions (Margins and CATchment Segmentation; Laruelle et al., 2013) (Fig. 12), where little information is available for quantifying the ocean CO_2 sink at the decadal scale and for evaluation of the anthropogenic CO_2 uptake (Regnier et al., 2013; Dai et al., 2022; Li et al., 2024). To explore the change in the observed properties in the coastal zones and have an idea of the long-term C_T trends, we selected the time series with at least 10 years of data

(Table 7, Fig. 13). Except at high latitudes (Greenland and Antarctic coastal zones), we observed a warming in coastal zones (Fig. S11). Changes in salinity are also identified (increase or decrease), and results of the trends are presented for salinity-normalized C_T at 34, 35, or 38 depending on the region. Although the interannual variability is large in coastal waters, sometimes linked to extreme events (e.g., river discharges), we observed an increase in N-C_T at most of the eight selected locations. The exceptions are the coastal zones in the Gulf of Lion near the river Rhône and near Tasmania in October.

In the Gulf of Lion, the new data in the coastal zone confirmed the first view at the SOLEMIO station over 2016–2018 (Bay of Marseille; Wimart-Rousseau et al., 2020). In this region the lowest C_T was observed in summer 2022 (average C_T of $2238.6 \pm 21.0\,\mu mol\,kg^{-1}$), much lower than in 2015 ($2290.8 \pm 44.7\,\mu mol\,kg^{-1}$). Over the continental shelf south of Tasmania (MARCATS no. 34), the trend in N-C_T was positive in summer but not significant in October. In October this was associated with an increase in salinity and in A_T probably linked to advective processes via the reversal and variability in the Zeehan or the East Australian currents. From our data a warming of $+0.06\,°C\,yr^{-1}$ was identified for both seasons over 2002–2012, as previously observed south of Tasmania over 1991–2003, impacting the pCO_2 trend and air–sea CO_2 fluxes in this region (Borges et al., 2008). The difference in the N–C_T trends in austral summer and spring calls for new detailed studies with extended data in this region. At high latitudes in Adélie Land (Antarctic coast MARCATS no. 45), the variability in N-C_T was large (range from 2150 to $2200\,\mu mol\,kg^{-1}$; Fig. 13), and the trend over 10 years in summer was not significant (Table 7). As opposed to the open zone at 60° S (Fig. 10), the C_T concentrations in the coastal zone near Antarctica did not increase, probably linked to competitive processes between anthropogenic uptake, changes in primary production, mixing, or ice melting (Shadwick et al., 2013, 2014). More data are needed to better evaluate the changes in the carbonate system in Antarctic coastal zones where bottom waters are formed and transport anthropogenic CO_2 at lower latitudes (Zhang et al., 2023).

For the coastal time series SOMLIT where annual trends could be estimated (sampling at monthly resolution), the N-C_T increase ($+2.1$ to $3.4\,\mu mol\,kg^{-1}\,yr^{-1}$) is close to or higher than the anthropogenic signal, leading to a decrease in pH ranging between -0.05 and -0.06 TS (total scale) per decade. The new data added to the SNAPO-CO_2-v2 dataset (2016–2023) confirm the progressive increase in C_T and the acidification in the western Mediterranean Sea and in the northeastern Atlantic coastal zones (Kapsenberg et al., 2017; Gac et al., 2021).

6 Data availability

Data presented in this study are available at SEANOE (https://www.seanoe.org, last access: 22 January 2025, https://doi.org/10.17882/102337, Metzl et al., 2024c). See also https://doi.org/10.17882/95414 (Metzl et al., 2024a) for version V1. The dataset is also available at https://explore.webodv.awi.de/ocean/carbon/snapo-co2/ (SNAPO-CO2, 2024).

7 Summary and suggestions

This work extends on the time and new oceanic regions of the A_T and C_T data presented in the first SNAPO-CO_2 synthesis (Metzl et al., 2024a). It includes now more than 67 000 surface and water column observations in all oceanic basins, in the Mediterranean Sea, in the coastal zones, near coral reefs, and in rivers. The data synthesized in version v2 are based on measurements of A_T and C_T performed between 1993 and 2023 with an accuracy of $\pm 4\,\mu mol\,kg^{-1}$. Based on a secondary quality control, 91 % of the A_T and C_T data are considered good (WOCE Flag 2) and 6 % probably good (Flag 3). For the open ocean this synthesis complements the SOCAT, GLODAP, and SPOTS data products (Bakker et al., 2016; Lauvset et al., 2024; Lange et al., 2024). For the coastal sites this also complements the synthesis of coastal time series in the Iberian Peninsula (Padin et al., 2020), on the Canadian Atlantic continental shelf (Gibb et al., 2023), and around North America (Fassbender et al., 2018; Jiang et al., 2021). The SNAPO-CO_2 dataset enables one to investigate the seasonal cycles, the interannual variability, and the decadal trends in A_T and C_T in various oceanic provinces. The same temporal analyses could be investigated for other carbonate system properties such as fCO_2 or pH calculated from A_T and C_T for air–sea CO_2 flux estimates or ocean acidification studies (Fig. 14).

In almost all regions the new data in 2021–2023 indicated that the C_T concentrations were higher in recent years. In regions where data are available for more than 2 decades, the time series show an increase in sea surface C_T (North Atlantic, southern Indian Ocean, and Ligurian Sea) with a rate close to or higher than the changes expected from anthropogenic CO_2 uptake. It is also recognized that at seasonal scale the C_T trends could be different. However, with the data in hand, the long-term trend in C_T cannot be quantified with confidence to compare with the anthropogenic carbon uptake in some regions. This is the case in the eastern tropical Atlantic, subject to high interannual variability (Lefèvre et al., 2021, 2024), although new data have been added over 2005–2022 in this region (Table 1, Fig. S9). When data are available for less than a decade, the increase in C_T was observed, but the trend was uncertain due to large interannual variability (e.g., Adélie Land). An exception was identified in the coastal zone in the Gulf of Lion (Mediterranean Sea) where summer data since 2010 present

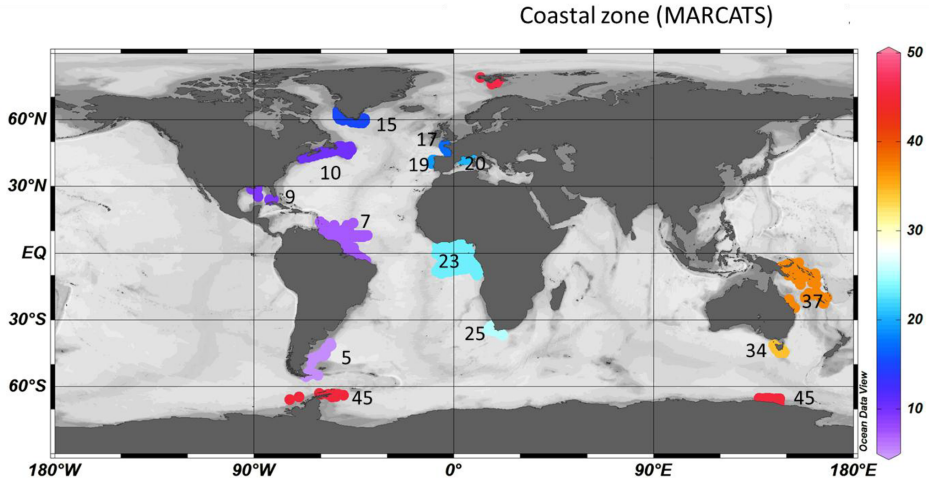

Figure 12. Location of A_T and C_T data available in the coastal zones in the SNAPO-CO_2-v2 dataset. Numbers and color code identify the MARCATS region (Laruelle et al., 2013). Figure produced with ODV (Schlitzer, 2018).

Table 7. Trends in N-C_T ($\mu mol\,kg^{-1}\,yr^{-1}$) and corresponding standard errors in selected coastal regions where data are available for 10 years or more. The projects/cruises for selection of the data in each domain are indicated. MARCATS regions nos. are also identified. Salinity values used for C_T normalization are indicated.

MARCATS region no.	Period	Season	N-C_T trend ($\mu mol\,kg^{-1}\,yr^{-1}$)	Salinity	Projects/cruises
Scotian no. 10	2002–2023	March–April	+1.71 (0.97)	35	SURATLANT
Greenland no. 15	2006–2023	June–mid-September	+5.77 (1.62)	35	OVIDE, SURATLANT
Roscoff no. 17	2010–2022	All seasons	+3.40 (0.76)	35	CHANNEL, COCORICO$_2$, SOMLIT ROSCOFF
Bay of Brest no. 17	2009–2022	All seasons	+2.17 (0.52)	35	SOMLIT-Brest, COCORICO$_2$, ECOSCOPA
Gulf of Lion no. 20	2010–2023	June–September	−1.19 (1.25)	38	COCORICO$_2$, MOOSE-GE, SOLEMIO*
Ligurian Sea no. 20	2008–2022	All seasons	+2.12 (0.36)	38	SOMLIT-Point-B, MOOSE-GE
Tasmania no. 34	2003–2013	January–February	+2.73 (1.72)	35	MINERVE, OISO
Tasmania no. 34	2002–2012	October	−0.65 (0.89)	35	MINERVE, OISO
Adélie no. 45	2002–2012	December–February	+0.63 (0.70)	34	MINERVE, OISO

* For LION, some data in summer were also used from punctual cruises: AMOR-BFlux, CARBORHONE, DICASE, LATEX, MESURHOBENT, MISSRHODIA-2, and MOLA.

a decrease in C_T, most pronounced since 2015 (C_T trend $= -5.2 \pm 1.5\,\mu mol\,kg^{-1}\,yr^{-1}$). Such a C_T decrease over 10 years was also observed in the Hawaii Ocean Time-series (HOT) over 2010–2020 (Dore et al., 2009, https://hahana.soest.hawaii.edu/hot/hotco2/hotco2.html, last access: 27 August 2024).

Although the A_T concentrations present significant interannual variability such as in the NASPG, in the tropical Atlantic or Adélie Land and coastal zones, A_T appears relatively constant over time except at some locations. In the open ocean, we observed an increase in A_T in the Southern Ocean south of the polar front around 60° S in 2003–2012 not directly linked to salinity. In the coastal zones a decrease in A_T was pronounced south of Greenland. On the coast in the Gulf of Lion, as observed for C_T, A_T decreased (A_T trend $= -2.8 \pm 1.2\,\mu mol\,kg^{-1}\,yr^{-1}$). This is opposed to the changes observed in the Ligurian Sea at station SOMLIT-Point-B, where C_T and A_T increased over 2007–2015 (Kapsenberg et al., 2017), highlighting the contrasting C_T and A_T trends in the Mediterranean coastal zones where ocean acidification is detected (here over 2008–2022, pH trend of -0.048 ± 0.003 per decade). With continuous warming, reduced stratification, and rapid pH change observed in the Mediterranean Sea, how the marine ecosystems will respond in the future should be addressed (e.g., Howes et al., 2015; Maugendre et al., 2015; Lacoue-Labarthe et al., 2016). The SNAPO-CO_2-v2 dataset could also be used to explore and analyze the changes in the carbonate system occurring during extreme events such as marine heat waves, rapid freshening, deep convection, and high-phytoplankton-bloom events.

This dataset could also serve for validating autonomous platforms capable of measuring pH and fCO_2 properties (Sarmiento et al., 2023); along with other synthesis products, it provides an additional reference dataset for the development and validation of regional biogeochemical models for simulating air–sea CO_2 fluxes. Thanks to the RECCAP2 stories, it has been recognized that ocean biogeochemical models present biases in the seasonal cycle of C_T and A_T due

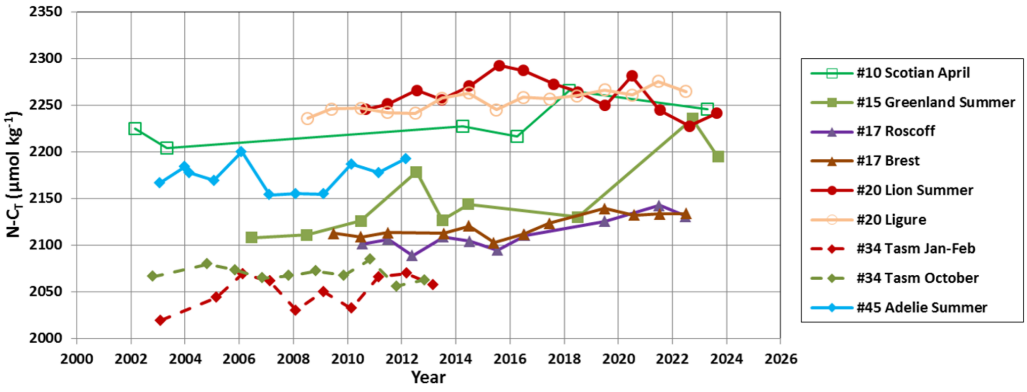

Figure 13. Time series of average N-C_T concentrations (µmol kg^{-1}) in selected MARCATS regions for different periods when data are available for 10 years or more. The trends and periods for each region are indicated in Table 7.

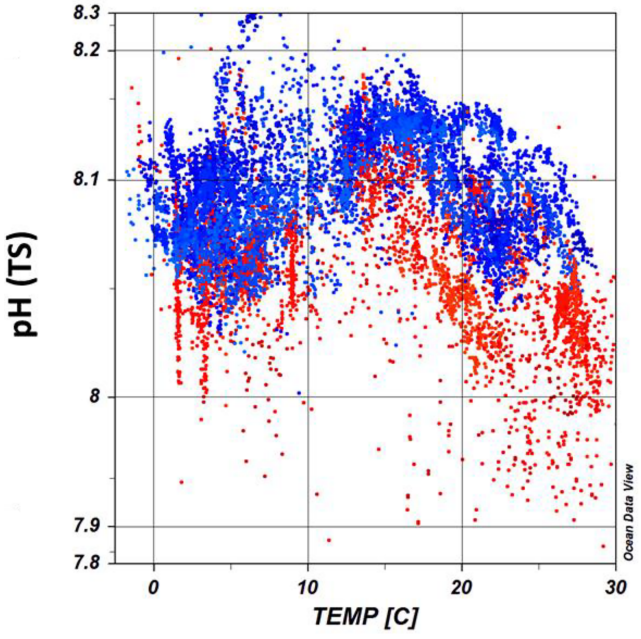

Figure 14. An example of observed ocean acidification derived from the SNAPO-CO_2-v2 dataset: pH (total scale) calculated with A_T and C_T data are presented as a function of temperature (°C) for years 1998–2002 (blue symbols) and 2020–2023 (red symbols) and for salinity > 33 (number of data selected with flag 2 = 11 994). In recent years the pH was lower. Figure produced with ODV (Schlitzer, 2018).

to inadequate representation of biogeochemical cycles (e.g., Hauck et al., 2023; Rodgers et al., 2023; Sarma et al., 2023; Pérez et al., 2024; Resplandy et al., 2024). The SNAPO-CO_2-v2 dataset could be used to guide analyses for regional or global biogeochemical models for A_T and C_T comparison and validation from seasonal to decadal scales. Our dataset is also essential for training and validating neural networks capable of predicting variables in the carbonate system (e.g., Fourrier et al., 2020; Chau et al., 2024a; Gregor et al., 2024), thereby enhancing observations of marine CO_2 at different spatial and temporal scales. Furthermore, we encourage the use of this dataset (or part of it), at sea or prior to going to sea for cruise planning. Indeed, using the approach of Davis and Goyet (2021), which takes into account the multiple constraints (e.g., ship time, number of samples), it is possible to determine the most appropriate sampling strategy (Guglielmi et al., 2022, 2023) to reach the specific scientific objectives of each cruise.

The data presented here are available online on the SEANOE server (https://doi.org/10.17882/102337, Metzl et al., 2024c) in a file identifying version v1 and v2. The sources of the original datasets (DOI) with the associated references are listed in the Supplement (Tables S3, S4). As for version v1 we invite the users to comment on any anomaly that would have not been detected or to suggest potential misqualification of data in the present product (e.g., data probably good albeit assigned with flag 3 are probably wrong). As for SOCAT or GLODAP, we expect to update the SNAPO-CO_2 dataset once new observations are obtained and controlled.

Supplement. The supplement related to this article is available online at https://doi.org/10.5194/essd-17-1075-2025-supplement.

Author contributions. NM prepared the data synthesis, prepared the figures, and wrote the draft of the manuscript with contributions from all authors. JF has measured the discrete samples since 2014, with the help of CM and CLM, and prepared the individual reports for each project. NM and JF prequalified the discrete A_T–C_T data. CLM and NM are co-investigators of the ongoing OISO project and qualified the underway A_T–C_T data from OISO cruises. FT and CG were PIs of the MINERVE cruises. All authors have contributed to organizing cruises, sample collection, and/or data qualification and reviewed the manuscript.

Competing interests. At least one of the (co-)authors is a member of the editorial board of *Earth System Science Data*. The peer-review process was guided by an independent editor, and the authors also have no other competing interests to declare.

Disclaimer. Publisher's note: Copernicus Publications remains neutral with regard to jurisdictional claims made in the text, published maps, institutional affiliations, or any other geographical representation in this paper. While Copernicus Publications makes every effort to include appropriate place names, the final responsibility lies with the authors.

Acknowledgements. Most of the A_T and C_T data presented in this study were measured at the SNAPO-CO_2 facility (Service National d'Analyse des Paramètres Océaniques du CO_2) housed by the LOCEAN laboratory and part of OSU ECCE Terra at Sorbonne University and INSU/CNRS analytical services. The support of INSU/CNRS, of OSU ECCE Terra, and of LOCEAN is gratefully acknowledged as well as the support of different French "Services nationaux d'Observations", such as OISO/CARAUS, SOMLIT, PIRATA, SSS, and MOOSE. We thank the research infrastructure of ICOS (Integrated Carbon Observation System), France, for funding a large part of the analyses. We thank the IRD (Institut de Recherche pour le Développement) and the French–Brazilian IRD–FAPEMA program for funding observations in the tropical Atlantic. We thank the French Oceanographic Fleet ("Flotte océanographique française") for financial and logistic support for most cruises listed in this synthesis and for the OISO program (https://campagnes.flotteoceanographique.fr/series/228/, last access: 22 January 2025). We acknowledge the MOOSE program (Mediterranean Ocean Observing System for the Environment, https://campagnes.flotteoceanographique.fr/series/235/fr/, last access: 22 January 2025) coordinated by CNRS-INSU and the research infrastructure of ILICO (CNRS-IFREMER). The CocoriCO_2 project was founded by European Maritime and Fisheries Fund (grant no. 344, 2020–2023) and benefited from a subsidy from the Adour-Garonne water agency. We thank the following programs coordinated by A. Tribollet, which have contributed to the acquisition of the data in Mayotte: CARBODISS funded by CNRS-INSU in 2018–2019, Future Maore reefs funded by Next Generation UE-France Relance in 2021–2023, and OA-ME funded by a Belmont Forum International (ANR) in 2020–2026. We thank the program Mermex-MISTRALS CNRS for supporting AMORBFlux, CARBORHONE, DICASE, and MESURHOBENT cruises and the program EC2CO-INSU for supporting the MISSRHODIA-2 cruise. The ACCESS project was supported by CNRS MISTRALS and the DELTARHONE1 by EC2CO-INSU. The ACIDHYPO project was founded by CNRS International Emerging Actions; we thank the captain and crew of R/V *Savannah* from the Skidaway Institute of Oceanography (University of Georgia) for their support and technical assistance during the operations at sea. The AMAZOMIX project was funded by French Oceanographic Fleet, INSU (LEFE), IRD (LMI TAPICOA), CNES (TOSCA MIAMAZ project), and the French–Brazilian international program GUYAMAZON. The OISO program was supported by the French institutes INSU (Institut National des Sciences de l'Univers), IPEV (Institut Polaire Paul-Émile Victor), and OSU Ecce-Terra (at Sorbonne Université) and the French program SOERE/Great-Gases. We also thank the research infrastructure at ILICO (https://www.ir-ilico.fr, last access: 22 January 2025). We warmly thank Alain Poisson, who initiated the MINERVE program and performed many of the measurements on board R/V *Astrolabe* from 2002 through 2018. We thank all colleagues and students who participated in the cruises and carefully collected the precious seawater samples. We thank Frédéric Merceur (IFREMER) for preparing the page and data availability on SEANOE and Reiner Schlitzer (AWI) for including the SNAPO-CO_2 dataset in the ODV portal. We thank the associate editor, Sebastiaan van de Velde, for managing this article and Kim Currie and Toste Tanhua for their suggestions that helped to improve this article.

Financial support. This research has been supported by the Institut national des sciences de l'Univers (SA/SNAPO-CO_2).

Review statement. This paper was edited by Sebastiaan van de Velde and reviewed by Kim Currie and Toste Tanhua.

References

Álvarez, M., Catalá, T. S., Civitarese, G., Coppola, L., Hassoun, A. E. R., Ibello, V., Lazzari, P., Lefèvre, D., Macías, D., Santinelli, C., and Ulses, C.: Chapter 11 – Mediterranean Sea general biogeochemistry, edited by: Schroeder, K. and Chiggiato, J., Oceanography of the Mediterranean Sea, Elsevier, 387–451, https://doi.org/10.1016/B978-0-12-823692-5.00004-2, 2023.

Bakker, D. C. E., Pfeil, B., Landa, C. S., Metzl, N., O'Brien, K. M., Olsen, A., Smith, K., Cosca, C., Harasawa, S., Jones, S. D., Nakaoka, S., Nojiri, Y., Schuster, U., Steinhoff, T., Sweeney, C., Takahashi, T., Tilbrook, B., Wada, C., Wanninkhof, R., Alin, S. R., Balestrini, C. F., Barbero, L., Bates, N. R., Bianchi, A. A., Bonou, F., Boutin, J., Bozec, Y., Burger, E. F., Cai, W.-J., Castle, R. D., Chen, L., Chierici, M., Currie, K., Evans, W., Featherstone, C., Feely, R. A., Fransson, A., Goyet, C., Greenwood, N., Gregor, L., Hankin, S., Hardman-Mountford, N. J., Harlay, J., Hauck, J., Hoppema, M., Humphreys, M. P., Hunt, C. W., Huss, B., Ibánhez, J. S. P., Johannessen, T., Keeling, R., Kitidis, V., Körtzinger, A., Kozyr, A., Krasakopoulou, E., Kuwata, A., Landschützer, P., Lauvset, S. K., Lefèvre, N., Lo Monaco, C., Manke, A., Mathis, J. T., Merlivat, L., Millero, F. J., Monteiro, P. M. S., Munro, D. R., Murata, A., Newberger, T., Omar, A. M., Ono, T., Paterson, K., Pearce, D., Pierrot, D., Robbins, L. L., Saito, S., Salisbury, J., Schlitzer, R., Schneider, B., Schweitzer, R., Sieger, R., Skjelvan, I., Sullivan, K. F., Sutherland, S. C., Sutton, A. J., Tadokoro, K., Telszewski, M., Tuma, M., van Heuven, S. M. A. C., Vandemark, D., Ward, B., Watson, A. J., and Xu, S.: A multidecade record of high-quality fCO_2 data in version 3 of the Surface Ocean CO_2 Atlas (SOCAT), Earth Syst. Sci. Data, 8, 383–413, https://doi.org/10.5194/essd-8-383-2016, 2016.

Barral, Q.-B., Zakardjian, B., Dumas, F., Garreau, P., Testor, P., and Beuvier, J.: Characterization of fronts in the Western Mediterranean with a special focus on the North Balearic Front, Prog. Oceanogr., 197, 102636, https://doi.org/10.1016/j.pocean.2021.102636, 2021.

Barré, L., Diaz, F., Wagener, T., Van Wambeke, F., Mazoyer, C., Yohia, C., and Pinazo, C.: Implementation and assessment of a model including mixotrophs and the carbonate cycle (Eco3M_MIX-CarbOx v1.0) in a highly dynamic Mediterranean coastal environment (Bay of Marseille, France) – Part 1: Evolution of ecosystem composition under limited light and nutrient conditions, Geosci. Model Dev., 16, 6701–6739, https://doi.org/10.5194/gmd-16-6701-2023, 2023.

Barré, L., Diaz, F., Wagener, T., Mazoyer, C., Yohia, C., and Pinazo, C.: Implementation and assessment of a model including mixotrophs and the carbonate cycle (Eco3M_MIX-CarbOx v1.0) in a highly dynamic Mediterranean coastal environment (Bay of Marseille, France) – Part 2: Towards a better representation of total alkalinity when modeling the carbonate system and air–sea CO_2 fluxes, Geosci. Model Dev., 17, 5851–5882, https://doi.org/10.5194/gmd-17-5851-2024, 2024.

Bittig, H. C., Steinhoff, T., Claustre, H., Fiedler, B., Williams, N. L., Sauzède, R., Körtzinger, A., and Gattuso, J.-P.: An Alternative to Static Climatologies: Robust Estimation of Open Ocean CO_2 Variables and Nutrient Concentrations From T, S, and O_2 Data Using Bayesian Neural Networks. Front. Mar. Sci. 5:328. https://doi.org/10.3389/fmars.2018.00328, 2018

Bonou, F., Medeiros, C., Noriega, C., Araujo, M., Aubains HounsouGbo, A., and Lefèvre, N.: A comparative study of total alkalinity and total inorganic carbon near tropical Atlantic coastal regions, J. Coast Conserv., 26, 31, https://doi.org/10.1007/s11852-022-00872-5, 2022.

Borges, A. V., Tilbrook, B., Metzl, N., Lenton, A., and Delille, B.: Inter-annual variability of the carbon dioxide oceanic sink south of Tasmania, Biogeosciences, 5, 141–155, https://doi.org/10.5194/bg-5-141-2008, 2008.

Bourgeois, T., Orr, J. C., Resplandy, L., Terhaar, J., Ethé, C., Gehlen, M., and Bopp, L.: Coastal-ocean uptake of anthropogenic carbon, Biogeosciences, 13, 4167–4185, https://doi.org/10.5194/bg-13-4167-2016, 2016.

Brandon, M., Goyet, C., Touratier, F., Lefèvre, N., Kestenare, E., and Morrow, R.: Spatial and temporal variability of the physical, carbonate and CO_2 properties in the Southern Ocean surface waters during austral summer (2005–2019), Deep-Sea Res. Pt. I, 187, 103836, https://doi.org/10.1016/j.dsr.2022.103836. 2022

Broullón, D., Pérez, F. F., Velo, A., Hoppema, M., Olsen, A., Takahashi, T., Key, R. M., Tanhua, T., González-Dávila, M., Jeansson, E., Kozyr, A., and van Heuven, S. M. A. C.: A global monthly climatology of total alkalinity: a neural network approach, Earth Syst. Sci. Data, 11, 1109–1127, https://doi.org/10.5194/essd-11-1109-2019, 2019.

Broullón, D., Pérez, F. F., Velo, A., Hoppema, M., Olsen, A., Takahashi, T., Key, R. M., Tanhua, T., Santana-Casiano, J. M., and Kozyr, A.: A global monthly climatology of oceanic total dissolved inorganic carbon: a neural network approach, Earth Syst. Sci. Data, 12, 1725–1743, https://doi.org/10.5194/essd-12-1725-2020, 2020.

Carter, B. R., Feely, R. A., Williams, N. L., Dickson, A. G., Fong, M. B., and Takeshita, Y.: Updated methods for global locally interpolated estimation of alkalinity, pH, and nitrate, Limnol. Oceanogr. Meth., 16, 119–131, https://doi.org/10.1002/lom3.10232, 2018.

Chau, T.-T.-T., Gehlen, M., Metzl, N., and Chevallier, F.: CMEMS-LSCE: a global, 0.25°, monthly reconstruction of the surface ocean carbonate system, Earth Syst. Sci. Data, 16, 121–160, https://doi.org/10.5194/essd-16-121-2024, 2024a.

Chau, T.-T.-T., Chevallier, F., and Gehlen, M.: Global analysis of surface ocean CO_2 fugacity and air-sea fluxes with low latency, Geophys. Res. Lett., 51, e2023GL106670, https://doi.org/10.1029/2023GL106670, 2024b.

Cheng, L. J., Abraham, J., Zhu, J., Trenberth, K. E., Fasullo, J., Boyer, T., Locarnini, R., Zhang, B., Yu, F. J., Wan, L. Y., Chen, X. R., Song, X. Z., Liu, Y. L., and Mann, M. E.: Record-setting ocean warmth continued in 2019, Adv. Atmos. Sci., 37, 137–142, https://doi.org/10.1007/s00376-020-9283-7, 2020.

Cheng, L., Abraham, J., Trenberth, K. E., Boyer, T., Mann, M. E., Zhu, J., Wang, F., Yu, F., Locarnini, R., Fasullo, J., Zheng, F., Li, Y., Zhang, B., Wan, L., Chen, X., Wang, D., Feng, L., Song, X., Liu, Y., Reseghetti, F., Simoncelli, S., Gouretski, V., Chen, G., Mishonov, A., Reagan, J., von Schuckmann, K., Pan, Y., Tan, Z., Zhu, Y., Wei, W., Li, G., Ren, Q., Cao, L., and Lu, Y.: New Record Ocean Temperatures and Related Climate Indicators in 2023, Adv. Atmos. Sci., 41, 1068–1082, https://doi.org/10.1007/s00376-024-3378-5, 2024.

Copin-Montégut, C.: Alkalinity and carbon budgets in the Mediterranean Sea, Global Biogeochem. Cy., 7, 915–925, 1993.

Coppola, L., Fourrier, M., Pasqueron de Fommervault, O., Poteau, A., Riquier, E. D., and Béguery, L.: Highresolution study of the air-sea CO_2 flux and net community oxygen production in the Ligurian Sea by a fleet of gliders, Front. Mar. Sci., 10, 1233845, https://doi.org/10.3389/fmars.2023.1233845, 2023.

Curbelo-Hernández, D., Pérez, F. F., González-Dávila, M., Gladyshev, S. V., González, A. G., González-Santana, D., Velo, A., Sokov, A., and Santana-Casiano, J. M.: Ocean acidification trends and carbonate system dynamics across the North Atlantic subpolar gyre water masses during 2009–2019, Biogeosciences, 21, 5561–5589, https://doi.org/10.5194/bg-21-5561-2024, 2024.

Currie, K. I., Reid, M. R., and Hunter, K. A.: Interannual variability of carbon dioxide draw-down by subantarctic surface water near New Zealand, Biogeochemistry, 104, 23–34, https://doi.org/10.1007/s10533-009-9355-3, 2011.

Cyronak, T., Santos, I. R., Erler, D. V., and Eyre, B. D.: Groundwater and porewater as major sources of alkalinity to a fringing coral reef lagoon (Muri Lagoon, Cook Islands), Biogeosciences, 10, 2467–2480, https://doi.org/10.5194/bg-10-2467-2013, 2013.

Dai, M., Su, J., Zhao, Y., Hofmann, E. E., Cao, Z., Cai, W.-J., Gan, J., Lacroix, F., Laruelle, G. G., Meng, F., Müller, J. D., Regnier, P. A. G., Wang, G., and Wang, Z.: Carbon Fluxes in the Coastal Ocean: Synthesis, Boundary Processes and Future Trends, Annu. Rev. Earth Pl. Sc., 50, 593–626, https://doi.org/10.1146/annurev-earth-032320-090746, 2022.

Davis, D. and Goyet, C.: Balanced Error Sampling with applications to ocean biogeochemical sampling, Collection études, Presses Universitaires de Perpignan, 224 pp., ISBN 978-2-35412-452-6, 2021.

Dickson, A. G., Sabine, C. L., and Christian, J. R.: Guide to best practices for ocean CO_2 measurements, North Pacific Marine Science Organization, Sidney, British Columbia, 191 pp., https://doi.org/10.25607/OBP-1342, 2007.

DOE: Handbook of Methods for Analysis of the Various Parameters of the Carbon Dioxide System in Seawater, version 2, edited by: Dickson, A. G. and Goyet, C., ORNL/CDIAC-74, https://doi.org/10.2172/10107773, 1994.

Doney, S. C., Fabry, V. J., Feely, R. A., and Kleypas, J. A., Ocean acidification: The other CO_2 problem, Annu. Rev. Mar. Sci., 1, 169–192, 10.1146/annurev.marine.010908.163834, 2009.

Doney, S. C., Busch, D. S., Cooley, S. R., and Kroeker, K. J.: The Impacts of Ocean Acidification on Marine Ecosystems and Reliant Human Communities, Annu. Rev. Environ. Resour., 45, 83–112, https://doi.org/10.1146/annurev-environ-012320-083019. 2020.

Dore, J. E., Lukas, R., Sadler, D. W., Church, M. J., and Karl, D. M.: Physical and biogeochemical modulation of ocean acidification in the central North Pacific, P. Natl. Acad. Sci. USA, 106, 12235–12240, https://doi.org/10.1073/pnas.0906044106, 2009.

Edmond, J. M.: High precision determination of titration alkalinity and total carbon dioxide content of sea water by potentiometric titration, Deep-Sea Res., 17, 737–750, https://doi.org/10.1016/0011-7471(70)90038-0, 1970.

Eyring, V., Righi, M., Lauer, A., Evaldsson, M., Wenzel, S., Jones, C., Anav, A., Andrews, O., Cionni, I., Davin, E. L., Deser, C., Ehbrecht, C., Friedlingstein, P., Gleckler, P., Gottschaldt, K.-D., Hagemann, S., Juckes, M., Kindermann, S., Krasting, J., Kunert, D., Levine, R., Loew, A., Mäkelä, J., Martin, G., Mason, E., Phillips, A. S., Read, S., Rio, C., Roehrig, R., Senftleben, D., Sterl, A., van Ulft, L. H., Walton, J., Wang, S., and Williams, K. D.: ESMValTool (v1.0) – a community diagnostic and performance metrics tool for routine evaluation of Earth system models in CMIP, Geosci. Model Dev., 9, 1747–1802, https://doi.org/10.5194/gmd-9-1747-2016, 2016.

Fabry, V. J., Seibel, B. A., Feely, R. A. and Orr, J. C.: Impacts of ocean acidification on marine fauna and ecosystem processes, ICES J. Mar. Sci., 65, 414–432, https://doi.org/10.1093/icesjms/fsn048, 2008.

Faranda, D., Pascale, S., and Bulut, B.: Persistent anticyclonic conditions and climate change exacerbated the exceptional 2022 European-Mediterranean drought, Environ. Res. Lett., 18, 034030, https://doi.org/10.1088/1748-9326/acbc37, 2023.

Fassbender, A. J., Alin, S. R., Feely, R. A., Sutton, A. J., Newton, J. A., Krembs, C., Bos, J., Keyzers, M., Devol, A., Ruef, W., and Pelletier, G.: Seasonal carbonate chemistry variability in marine surface waters of the US Pacific Northwest, Earth Syst. Sci. Data, 10, 1367–1401, https://doi.org/10.5194/essd-10-1367-2018, 2018.

Fay, A. R. and McKinley, G. A.: Global open-ocean biomes: mean and temporal variability, Earth Syst. Sci. Data, 6, 273–284, https://doi.org/10.5194/essd-6-273-2014, 2014.

Fourrier, M., Coppola, L., Claustre, H., D'Ortenzio, F., Sauzède, R., and Gattuso, J.-P.: A regional neural network approach to estimate water-column nutrient concentrations and carbonate system variables in the Mediterranean Sea: CANYON-MED, Front. Mar. Sci., 7, 620, https://doi.org/10.3389/fmars.2020.00620, 2020.

Friedlingstein, P., O'Sullivan, M., Jones, M. W., Andrew, R. M., Gregor, L., Hauck, J., Le Quéré, C., Luijkx, I. T., Olsen, A., Peters, G. P., Peters, W., Pongratz, J., Schwingshackl, C., Sitch, S., Canadell, J. G., Ciais, P., Jackson, R. B., Alin, S. R., Alkama, R., Arneth, A., Arora, V. K., Bates, N. R., Becker, M., Bellouin, N., Bittig, H. C., Bopp, L., Chevallier, F., Chini, L. P., Cronin, M., Evans, W., Falk, S., Feely, R. A., Gasser, T., Gehlen, M., Gkritzalis, T., Gloege, L., Grassi, G., Gruber, N., Gürses, Ö., Harris, I., Hefner, M., Houghton, R. A., Hurtt, G. C., Iida, Y., Ilyina, T., Jain, A. K., Jersild, A., Kadono, K., Kato, E., Kennedy, D., Klein Goldewijk, K., Knauer, J., Korsbakken, J. I., Landschützer, P., Lefèvre, N., Lindsay, K., Liu, J., Liu, Z., Marland, G., Mayot, N., McGrath, M. J., Metzl, N., Monacci, N. M., Munro, D. R., Nakaoka, S.-I., Niwa, Y., O'Brien, K., Ono, T., Palmer, P. I., Pan, N., Pierrot, D., Pocock, K., Poulter, B., Resplandy, L., Robertson, E., Rödenbeck, C., Rodriguez, C., Rosan, T. M., Schwinger, J., Séférian, R., Shutler, J. D., Skjelvan, I., Steinhoff, T., Sun, Q., Sutton, A. J., Sweeney, C., Takao, S., Tanhua, T., Tans, P. P., Tian, X., Tian, H., Tilbrook, B., Tsujino, H., Tubiello, F., van der Werf, G. R., Walker, A. P., Wanninkhof, R., Whitehead, C., Willstrand Wranne, A., Wright, R., Yuan, W., Yue, C., Yue, X., Zaehle, S., Zeng, J., and Zheng, B.: Global Carbon Budget 2022, Earth Syst. Sci. Data, 14, 4811–4900, https://doi.org/10.5194/essd-14-4811-2022, 2022.

Friedlingstein, P., O'Sullivan, M., Jones, M. W., Andrew, R. M., Bakker, D. C. E., Hauck, J., Landschützer, P., Le Quéré, C., Luijkx, I. T., Peters, G. P., Peters, W., Pongratz, J., Schwingshackl, C., Sitch, S., Canadell, J. G., Ciais, P., Jackson, R. B., Alin, S. R., Anthoni, P., Barbero, L., Bates, N. R., Becker, M., Bellouin, N., Decharme, B., Bopp, L., Brasika, I. B. M., Cadule, P., Chamberlain, M. A., Chandra, N., Chau, T.-T.-T., Chevallier, F., Chini, L. P., Cronin, M., Dou, X., Enyo, K., Evans, W., Falk, S., Feely, R. A., Feng, L., Ford, D. J., Gasser, T., Ghattas, J., Gkritzalis, T., Grassi, G., Gregor, L., Gruber, N., Gürses, Ö., Harris, I., Hefner, M., Heinke, J., Houghton, R. A., Hurtt, G. C., Iida, Y., Ilyina, T., Jacobson, A. R., Jain, A., Jarníková, T., Jersild, A., Jiang, F., Jin, Z., Joos, F., Kato, E., Keeling, R. F., Kennedy, D., Klein Goldewijk, K., Knauer, J., Korsbakken, J. I., Körtzinger, A., Lan, X., Lefèvre, N., Li, H., Liu, J., Liu, Z., Ma, L., Marland, G., Mayot, N., McGuire, P. C., McKinley, G. A., Meyer, G., Morgan, E. J., Munro, D. R., Nakaoka, S.-I., Niwa, Y., O'Brien, K. M., Olsen, A., Omar, A. M., Ono, T., Paulsen, M., Pierrot, D., Pocock, K., Poulter, B., Powis, C. M., Rehder, G., Resplandy, L., Robertson, E., Rödenbeck, C., Rosan, T. M., Schwinger, J., Séférian, R., Smallman, T. L., Smith, S. M., Sospedra-Alfonso, R., Sun, Q., Sutton, A. J., Sweeney, C., Takao, S., Tans, P. P., Tian, H., Tilbrook, B., Tsujino, H., Tubiello, F., van der Werf, G. R., van Ooijen, E., Wanninkhof, R., Watanabe, M., Wimart-Rousseau, C., Yang, D., Yang, X., Yuan, W., Yue, X., Zaehle, S., Zeng, J., and Zheng, B.: Global Carbon Budget 2023, Earth Syst. Sci. Data, 15, 5301–5369, https://doi.org/10.5194/essd-15-5301-2023, 2023.

Fröb, F., Olsen, A., Becker, M., Chafik, L., Johannessen, T., Reverdin, G., and Omar, A.: Wintertime fCO_2 variability in the subpolar North Atlantic since 2004, Geophys. Res. Lett., 46, 1580–1590, https://doi.org/10.1029/2018GL080554, 2019.

Gac, J.-P., Marrec, P., Cariou, T., Grosstefan, E., Macé, E., Rimmelin-Maury, P., Vernet, M., and Bozec, Y.: Decadal Dynamics of the CO_2 System and Associated Ocean Acidification in Coastal Ecosystems of the North East Atlantic Ocean, Front. Mar. Sci., 8, 688008, https://doi.org/10.3389/fmars.2021.688008, 2021.

Gallego, M. A., Timmermann, A., Friedrich, T., and Zeebe, R. E.: Drivers of future seasonal cycle changes in oceanic pCO_2, Biogeosciences, 15, 5315–5327, https://doi.org/10.5194/bg-15-5315-2018, 2018.

Gattuso, J.-P., Magnan, A., Billé, R., Cheung, W. W. L., Howes, E. L., Joos, F., Allemand, D., Bopp, L., Cooley, S., Eakin,

M., Hoegh-Guldberg, O., Kelly, R. P., Pörtner, H.-O., Rogers, A. D., Baxter, J. M., Laffoley, D., Osborn, D., Rankovic, A., Rochette, J., Sumaila, U. R., Treyer, S., and Turley, C.: Contrasting futures for ocean and society from different anthropogenic CO_2 emissions scenarios, Science, 349, aac4722, https://doi.org/10.1126/science.aac4722, 2015.

Gibb, O., Cyr, F., Azetsu-Scott, K., Chassé, J., Childs, D., Gabriel, C.-E., Galbraith, P. S., Maillet, G., Pepin, P., Punshon, S., and Starr, M.: Spatiotemporal variability in pH and carbonate parameters on the Canadian Atlantic continental shelf between 2014 and 2022, Earth Syst. Sci. Data, 15, 4127–4162, https://doi.org/10.5194/essd-15-4127-2023, 2023.

Goyet, C., Beauverger, C., Brunet, C., and Poisson, A.: Distribution of carbon dioxide partial pressure in surface waters of the Southwest Indian Ocean, Tellus B, 43, 1–11, https://doi.org/10.3402/tellusb.v43i1.15242, 1991.

Goyet, C., Hassoun, A. E. R. Gemayel, E. Touratier, F., Abboud-Abi Saab M. and Guglielmi, V.: Thermodynamic forecasts of the Mediterranean Sea Acidification, Mediterr. Mar. Sci., 17/2, 508–518, https://doi.org/10.12681/mms.1487, 2016.

Goyet C., Benallal, M.A., Bijoux A., Guglielmi, V, Moussa, H., Ribou, A.-C., and Touratier, F.: Ch.39, Evolution of human Impact on Oceans: Tipping points of socio-ecological Coviability, in: Coviability of Social and Ecological Systems: Reconnecting Mankind to the Biosphere in an Era of Global Change, edited by: Barrière, O., Behnassi, M., David, G., Douzal, V., Fargette, M., Libourel, T., Loireau, M., Pascal, L., Prost, C., Ravena-Cañete, V., Seyler, F., and Morand, S., Springer International Publishing AG, https://doi.org/10.1007/978-3-319-78111-2_12, 2019.

Gregor, L. and Gruber, N.: OceanSODA-ETHZ: a global gridded data set of the surface ocean carbonate system for seasonal to decadal studies of ocean acidification, Earth Syst. Sci. Data, 13, 777–808, https://doi.org/10.5194/essd-13-777-2021, 2021.

Gregor, L., Shutler, J., and Gruber, N. : High-resolution variability of the ocean carbon sink, Global Biogeochem. Cy., 38, e2024GB008127, https://doi.org/10.1029/2024GB008127, 2024.

Gruber, N., Clement, D., Carter, B. R., Feely, R. A., van Heuven, S., Hoppema, M., Ishii, M., Key, R. M., Kozyr, A., Lauvset, S. K., Lo Monaco, C., Mathis, J. T., Murata, A., Olsen, A., Perez, F. F., Sabine, C. L., Tanhua, T., and Wanninkhof, R.: The oceanic sink for anthropogenic CO_2 from 1994 to 2007, Science, 363, 1193–1199, https://doi.org/10.1126/science.aau5153, 2019.

Guglielmi, V., Touratier, F., and Goyet, C.: Design of sampling strategy measurements of CO_2/carbonate properties, J. Oceanogr. Aqua., 6, 1–11, https://doi.org/10.23880/ijoac-16000227, 2022.

Guglielmi, V., Touratier, F., and Goyet, C.: Determination of discrete sampling locations minimizing both the number of samples and the maximum interpolation error: Application to measurements of carbonate chemistry in surface ocean, J. Sea Res., 191, 102336, https://doi.org/10.1016/j.seares.2023.102336, 2023.

Hauck, J., Gregor, L., Nissen, C., Patara, L., Hague, M., Mongwe, P., Bushinsky, S., Doney, S. C., Gruber, N., Le Quéré, C., Manizza, M., Mazloff, M., Monteiro, P. M. S., and Terhaar, J.: The Southern Ocean carbon cycle 1985–2018: Mean, seasonal cycle, trends, and storage, Global Biogeochem. Cy., 37, e2023GB007848, https://doi.org/10.1029/2023GB007848, 2023.

Ho, D. T., Bopp, L., Palter, J. B., Long, M. C., Boyd, P. W., Neukermans, G., and Bach, L. T.: Monitoring, reporting, and verification for ocean alkalinity enhancement, in: Guide to Best Practices in Ocean Alkalinity Enhancement Research, edited by: Oschlies, A., Stevenson, A., Bach, L. T., Fennel, K., Rickaby, R. E. M., Satterfield, T., Webb, R., and Gattuso, J.-P., Copernicus Publications, State Planet, 2-oae2023, 12, https://doi.org/10.5194/sp-2-oae2023-12-2023, 2023.

Holliday, N. P., Bersch, M., Berx, B., Chafik, L., Cunningham, S., Florindo-López, C., Hátún, H., Johns, W., Josey, S. A., Larsen, K. M. H., Mulet, S., Oltmanns, M., Reverdin, G., Rossby, T., Thierry, V., Valdimarsson, H., and Yashayaev, I.: Ocean circulation causes the largest freshening event for 120 years in eastern subpolar North Atlantic, Nat. Commun., 11, 585, https://doi.org/10.1038/s41467-020-14474-y, 2020.

Howes, E., Stemmann, L., Assailly, C., Irisson, J.-O., Dima, M., Bijma, J., and Gattuso, J.-P.: Pteropod time series from the North Western Mediterranean (1967–2003): impacts of pH and climate variability, Mar. Ecol. Prog. Ser., 531, 193–206, https://doi.org/10.3354/meps11322, 2015.

IPCC: Changing Ocean, Marine Ecosystems, and Dependent Communities, in: The Ocean and Cryosphere in a Changing Climate, Cambridge University Press, 447–588, https://doi.org/10.1017/9781009157964.007, 2022.

Jiang, L.-Q., Feely, R. A., Wanninkhof, R., Greeley, D., Barbero, L., Alin, S., Carter, B. R., Pierrot, D., Featherstone, C., Hooper, J., Melrose, C., Monacci, N., Sharp, J. D., Shellito, S., Xu, Y.-Y., Kozyr, A., Byrne, R. H., Cai, W.-J., Cross, J., Johnson, G. C., Hales, B., Langdon, C., Mathis, J., Salisbury, J., and Townsend, D. W.: Coastal Ocean Data Analysis Product in North America (CODAP-NA) – an internally consistent data product for discrete inorganic carbon, oxygen, and nutrients on the North American ocean margins, Earth Syst. Sci. Data, 13, 2777–2799, https://doi.org/10.5194/essd-13-2777-2021, 2021.

Jiang, L., Dunne, J., Carter, B. R., Tjiputra, J. F., Terhaar, J., Sharp, J. D., Olsen, A., Alin, S., Bakker, D. C., Feely, R. A., Gattuso, J., Hogan, P., Ilyina, T., Lange, N., Lauvset, S. K., Lewis, E. R., Lovato, T., Palmieri, J., Santana-Falcón, Y., Schwinger, J., Séférian, R., Strand, G., Swart, N., Tanhua, T., Tsujino, H., Wanninkhof, R., Watanabe, M., Yamamoto, A., and Ziehn, T.: Global surface ocean acidification indicators from 1750 to 2100, J. Adv. Model. Earth Sy., 15, e2022MS003563, https://doi.org/10.1029/2022MS003563, 2023.

Jiang, Z.-P., Tyrrell, T., Hydes, D. J., Dai, M., and Hartman, S. E.: Variability of alkalinity and the alkalinity-salinity relationship in the tropical and subtropical surface ocean, Global Biogeochem. Cy., 28, 729–742, https://doi.org/10.1002/2013GB004678, 2014.

Jing, Y., Li, Y., Xu, Y., and Fan, G.: Influences of the NAO on the North Atlantic CO_2 fluxes in winter and summer on the interannual scale, Adv. Atmos. Sci., 36, 1288–1298, https://doi.org/10.1007/s00376-019-8247-2, 2019.

Kapsenberg, L., Alliouane, S., Gazeau, F., Mousseau, L., and Gattuso, J.-P.: Coastal ocean acidification and increasing total alkalinity in the northwestern Mediterranean Sea, Ocean Sci., 13, 411–426, https://doi.org/10.5194/os-13-411-2017, 2017.

Khatiwala, S., Tanhua, T., Mikaloff Fletcher, S., Gerber, M., Doney, S. C., Graven, H. D., Gruber, N., McKinley, G. A., Murata, A., Ríos, A. F., and Sabine, C. L.: Global ocean stor-

age of anthropogenic carbon, Biogeosciences, 10, 2169–2191, https://doi.org/10.5194/bg-10-2169-2013, 2013.

Koffi, U., Lefèvre, N., Kouadio, G., and Boutin, J.: Surface CO_2 parameters and air-sea CO_2 fluxes distribution in the eastern equatorial Altantic Ocean, J. Marine Syst., 82, 135–144, https://doi.org/10.1016/j.jmarsys/2010.04.010, 2010.

Kwiatkowski, L., Torres, O., Bopp, L., Aumont, O., Chamberlain, M., Christian, J. R., Dunne, J. P., Gehlen, M., Ilyina, T., John, J. G., Lenton, A., Li, H., Lovenduski, N. S., Orr, J. C., Palmieri, J., Santana-Falcón, Y., Schwinger, J., Séférian, R., Stock, C. A., Tagliabue, A., Takano, Y., Tjiputra, J., Toyama, K., Tsujino, H., Watanabe, M., Yamamoto, A., Yool, A., and Ziehn, T.: Twenty-first century ocean warming, acidification, deoxygenation, and upper-ocean nutrient and primary production decline from CMIP6 model projections, Biogeosciences, 17, 3439–3470, https://doi.org/10.5194/bg-17-3439-2020, 2020.

Lacoue-Labarthe, T., Nunes, P. A. L. D., Ziveri, P., Cinar, M., Gazeau, F., Hall-Spencer, J. M., Hilmi, N., Moschella, P., Safa, A., Sauzade, D., and Turley, C.: Impacts of ocean acidification in a warming Mediterranean Sea: An overview, Reg. Stud. Mar. Sci., 5, 1–11, https://doi.org/10.1016/j.rsma.2015.12.005, 2016.

Lagoutte, E., Tribollet, A., Bureau, S., Cordier, E., Mangion, P., Chauvin, A., Mouquet, P., Bigot, L., Frouin, P., and Cuet, P.: Biogeochemical evidence of flow re-entrainment on the main fringing reef of La Reunion Island, Mar. Chem., 259, 104352, https://doi.org/10.1016/j.marchem.2024.104352, 2023.

Laika, H. E., Goyet, C., Vouve, F., Poisson, A., and Touratier, F.: Interannual properties of the CO_2 system in the Southern Ocean south of Australia, Antarctic Sci., 21, 663–680, https://doi.org/10.1017/S0954102009990319, 2009.

Lan, X., Tans, P., and Thoning, K. W.: Trends in globally-averaged CO_2 determined from NOAA Global Monitoring Laboratory measurements, Version 2024-08, https://doi.org/10.15138/9N0H-ZH07, 2024.

Landschützer, P., Gruber, N., Bakker, D. C. E., Stemmler, I., and Six, K. D.: Strengthening seasonal marine CO_2 variations due to increasing atmospheric CO_2, Nat. Clim. Change, 8, 146–150, https://doi.org/10.1038/s41558-017-0057-x, 2018.

Landschützer, P., Ilyina, T., and Lovenduski, N. S.: Detecting regional modes of variability in observation-based surface ocean pCO_2, Geophys. Res. Lett., 46, 2670–2679, https://doi.org/10.1029/2018GL081756, 2019

Lange, N., Fiedler, B., Álvarez, M., Benoit-Cattin, A., Benway, H., Buttigieg, P. L., Coppola, L., Currie, K., Flecha, S., Gerlach, D. S., Honda, M., Huertas, I. E., Lauvset, S. K., Muller-Karger, F., Körtzinger, A., O'Brien, K. M., Ólafsdóttir, S. R., Pacheco, F. C., Rueda-Roa, D., Skjelvan, I., Wakita, M., White, A., and Tanhua, T.: Synthesis Product for Ocean Time Series (SPOTS) – a ship-based biogeochemical pilot, Earth Syst. Sci. Data, 16, 1901–1931, https://doi.org/10.5194/essd-16-1901-2024, 2024.

Laruelle, G. G., Dürr, H. H., Lauerwald, R., Hartmann, J., Slomp, C. P., Goossens, N., and Regnier, P. A. G.: Global multi-scale segmentation of continental and coastal waters from the watersheds to the continental margins, Hydrol. Earth Syst. Sci., 17, 2029–2051, https://doi.org/10.5194/hess-17-2029-2013, 2013.

Laruelle, G. G., Cai, W.-J., Hu, X., Gruber, N., Mackenzie, F. T., and Regnier, P.: Continental shelves as a variable but increasing global sink for atmospheric carbon dioxide, Nat. Commun., 9, 454, https://doi.org/10.1038/s41467-017-02738-z, 2018.

Lauvset, S. K., Lange, N., Tanhua, T., Bittig, H. C., Olsen, A., Kozyr, A., Álvarez, M., Azetsu-Scott, K., Brown, P. J., Carter, B. R., Cotrim da Cunha, L., Hoppema, M., Humphreys, M. P., Ishii, M., Jeansson, E., Murata, A., Müller, J. D., Pérez, F. F., Schirnick, C., Steinfeldt, R., Suzuki, T., Ulfsbo, A., Velo, A., Woosley, R. J., and Key, R. M.: The annual update GLODAPv2.2023: the global interior ocean biogeochemical data product, Earth Syst. Sci. Data, 16, 2047–2072, https://doi.org/10.5194/essd-16-2047-2024, 2024.

Lefèvre, N., Flores Montes, M., Gaspar, F. L., Rocha, C., Jiang, S., De Araújo, M. C., and Ibánhez, J. S. P.: Net Heterotrophy in the Amazon Continental Shelf Changes Rapidly to a Sink of CO_2 in the Outer Amazon Plume, Front. Mar. Sci., 4, 278, https://doi.org/10.3389/fmars.2017.00278, 2017.

Lefèvre, N., Mejia, C., Khvorostyanov, D., Beaumont, L., and Koffi, U.: Ocean Circulation Drives the Variability of the Carbon System in the Eastern Tropical Atlantic, Oceans, 2, 126–148, https://doi.org/10.3390/oceans2010008, 2021.

Lefèvre, N., Veleda, D., and Beaumont, L.: Trends and drivers of CO_2 parameters, from 2006 to 2021, at a time-series station in the Eastern Tropical Atlantic (6° S, 10° W), Front. Mar. Sci. 11, 1299071, https://doi.org/10.3389/fmars.2024.1299071, 2024.

Leseurre, C., Lo Monaco, C., Reverdin, G., Metzl, N., Fin, J., Olafsdottir, S., and Racapé, V.: Ocean carbonate system variability in the North Atlantic Subpolar surface water (1993–2017), Biogeosciences, 17, 2553–2577, https://doi.org/10.5194/bg-17-2553-2020, 2020.

Leseurre, C., Lo Monaco, C., Reverdin, G., Metzl, N., Fin, J., Mignon, C., and Benito, L.: Summer trends and drivers of sea surface fCO_2 and pH changes observed in the southern Indian Ocean over the last two decades (1998–2019), Biogeosciences, 19, 2599–2625, https://doi.org/10.5194/bg-19-2599-2022, 2022.

Li, X., Wu, Z., Ouyang, Z., and Cai, W.-J. : The source and accumulation of anthropogenic carbon in the U.S. East Coast, Sci. Adv., 10, eadl3169, https://doi.org/10.1126/sciadv.adl3169, 2024.

Mathis, M., Lacroix, F., Hagemann, S., Nielsen, D. M., Ilyina, T., and Schrum, C.: Enhanced CO_2 uptake of the coastal ocean is dominated by biological carbon fixation, Nat. Clim. Chang., 14, 373–379, https://doi.org/10.1038/s41558-024-01956-w, 2024.

Maugendre, L., Gattuso, J.-P., Louis, J., de Kluijver, A., Marro, S., Soetaert, K., and Gazeau, F.: Effect of ocean warming and acidification on a plankton community in the NW Mediterranean Sea, ICES J. Mar. Sci., 72, 1744–1755, https://doi.org/10.1093/icesjms/fsu161, 2015.

Mercier, H., Lherminier, P., Sarafanov, A., Gaillard, F., Daniault, N., Desbruyères, D., Falina, A., Ferron, B., Huck, T., and Thierry, V.: Variability of the meridional overturning circulation at the Greenland-Portugal Ovide section from 1993 to 2010, Prog. Oceanogr., 132, 250–261, https://doi.org/10.1016/j.pocean.2013.11.001, 2015.

Mercier, H., Desbruyères, D., Lherminier, P., Velo, A., Carracedo, L., Fontela, M., and Pérez, F. F.: New insights into the eastern subpolar North Atlantic meridional overturning circulation from OVIDE, Ocean Sci., 20, 779–797, https://doi.org/10.5194/os-20-779-2024, 2024.

Metzl, N., Brunet, C., Jabaud-Jan, A., Poisson, A., and Schauer, B.: Summer and winter air-sea CO_2 fluxes in the Southern Ocean, Deep-Sea Res. Pt. I, 53, 1548–1563, https://doi.org/10.1016/j.dsr.2006.07.006, 2006.

Metzl, N., Corbière, A., Reverdin, G., Lenton, A., Takahashi, T., Olsen, A., Johannessen, T., Pierrot, D., Wanninkhof, R., Ólafsdóttir, S. R., Olafsson, J., and Ramonet, M.: Recent acceleration of the sea surface fCO_2 growth rate in the North Atlantic subpolar gyre (1993–2008) revealed by winter observations, Global Biogeochem. Cy., 24, GB4004, https://doi.org/10.1029/2009GB003658, 2010.

Metzl, N., Lo Monaco, C., Leseurre, C., Ridame, C., Fin, J., Mignon, C., Gehlen, M., and Chau, T. T. T.: The impact of the South-East Madagascar Bloom on the oceanic CO_2 sink, Biogeosciences, 19, 1451–1468, https://doi.org/10.5194/bg-19-1451-2022, 2022.

Metzl, N., Fin, J., Lo Monaco, C., Mignon, C., Alliouane, S., Antoine, D., Bourdin, G., Boutin, J., Bozec, Y., Conan, P., Coppola, L., Diaz, F., Douville, E., Durrieu de Madron, X., Gattuso, J.-P., Gazeau, F., Golbol, M., Lansard, B., Lefèvre, D., Lefèvre, N., Lombard, F., Louanchi, F., Merlivat, L., Olivier, L., Petrenko, A., Petton, S., Pujo-Pay, M., Rabouille, C., Reverdin, G., Ridame, C., Tribollet, A., Vellucci, V., Wagener, T., and Wimart-Rousseau, C.: A synthesis of ocean total alkalinity and dissolved inorganic carbon measurements from 1993 to 2022: the SNAPO-CO_2-v1 dataset, Earth Syst. Sci. Data, 16, 89–120, https://doi.org/10.5194/essd-16-89-2024, 2024a.

Metzl, N., Lo Monaco, C., Leseurre, C., Ridame, C., Reverdin, G., Chau, T. T. T., Chevallier, F., and Gehlen, M.: Anthropogenic CO_2, air–sea CO_2 fluxes, and acidification in the Southern Ocean: results from a time-series analysis at station OISO-KERFIX (51° S–68° E), Ocean Sci., 20, 725–758, https://doi.org/10.5194/os-20-725-2024, 2024b.

Metzl, N., Fin, J., Lo Monaco, C., Mignon, C., Alliouane, S., Bombled, B., Boutin, J., Bozec, Y., Comeau, S., Conan, P., Coppola, L., Cuet, P., Ferreira, E., Gattuso, J.-P., Gazeau, F., Goyet, C., Grossteffan, E., Lansard, B., Lefèvre, D., Lefèvre, N., Leseurre, C., Lombard, F., Petton, S., Pujo-Pay, M., Rabouille, C., Reverdin, G., Ridame, C., Rimmelin-Maury, P., Ternon, J.-F., Touratier, F., Tribollet, A., Wagener, T., and Wimart-Rousseau, C.: An updated synthesis of ocean total alkalinity and dissolved inorganic carbon measurements from 1993 to 2023: the SNAPO-CO_2-v2 dataset, SEANOE [data set], https://doi.org/10.17882/102337, 2024c.

Metzl, N., Lo Monaco, C., Barut, G., and Ternon, J.-F.: Contrasting trends of the ocean CO_2 sink and pH in the Agulhas current system and the Mozambique Basin, South-Western Indian Ocean (1963–2023), Deep-Sea Res. Pt. II, 220, 105459, https://doi.org/10.1016/j.dsr2.2025.105459, 2025.

Mu, L., Gomes, H. do R., Burns, S. M., Goes, J. I., Coles, V. J., Rezende, C. E., Thompson, F. L., Moura, R. L., Page, B., and Yager, P. L.: Temporal Variability of Air-Sea CO_2 flux in the Western Tropical North Atlantic Influenced by the Amazon River Plume, Global Biogeochem. Cy., 35, e2020GB006798, https://doi.org/10.1029/2020GB006798, 2021.

Munro, D. R., Lovenduski, N. S., Takahashi, T., Stephens, B. B., Newberger, T., and Sweeney, C.: Recent evidence for a strengthening CO_2 sink in the Southern Ocean from carbonate system measurements in the Drake Passage (2002–2015), Geophys. Res. Lett., 42, 7623–7630, https://doi.org/10.1002/2015GL065194, 2015.

Müller, J. D., Gruber, N., Carter, B., Feely, R., Ishii, M., Lange, N., Lauvset, S. K., Murata, A., Olsen, A., Pérez, F. F., Sabine, C., Tanhua, T., Wanninkhof, R., and Zhu, D.: Decadal trends in the oceanic storage of anthropogenic carbon from 1994 to 2014, AGU Adv., 4, e2023AV000875, https://doi.org/10.1029/2023AV000875, 2023.

Newton, J. A., Feely, R. A., Jewett, E. B., Williamson, P., and Mathis, J.: Global Ocean Acidification Observing Network: Requirements and Governance Plan, 2nd Edn., GOA-ON, https://www.iaea.org/sites/default/files/18/06/goa-on-second-edition-2015.pdf (last access: 22 January 2025), 2015.

Olafsson, J., Olafsdottir, S. R., Benoit-Cattin, A., and Takahashi, T.: The Irminger Sea and the Iceland Sea time series measurements of sea water carbon and nutrient chemistry 1983–2008, Earth Syst. Sci. Data, 2, 99–104, https://doi.org/10.5194/essd-2-99-2010, 2010.

Olivier, L., Boutin, J., Reverdin, G., Lefèvre, N., Landschützer, P., Speich, S., Karstensen, J., Labaste, M., Noisel, C., Ritschel, M., Steinhoff, T., and Wanninkhof, R.: Wintertime process study of the North Brazil Current rings reveals the region as a larger sink for CO_2 than expected, Biogeosciences, 19, 2969–2988, https://doi.org/10.5194/bg-19-2969-2022, 2022.

Olsen, A., Key, R. M., van Heuven, S., Lauvset, S. K., Velo, A., Lin, X., Schirnick, C., Kozyr, A., Tanhua, T., Hoppema, M., Jutterström, S., Steinfeldt, R., Jeansson, E., Ishii, M., Pérez, F. F., and Suzuki, T.: The Global Ocean Data Analysis Project version 2 (GLODAPv2) – an internally consistent data product for the world ocean, Earth Syst. Sci. Data, 8, 297–323, https://doi.org/10.5194/essd-8-297-2016, 2016.

Oudot, C., Ternon, J. F., and Lecomte, J.: Measurements of atmospheric and oceanic CO_2 in the tropical Atlantic: 10 years after the 1982–1984 FOCAL cruises, Tellus B, 47, 70–85, https://doi.org/10.3402/tellusb.v47i1-2.16032, 1995

Padin, X. A., Velo, A., and Pérez, F. F.: ARIOS: a database for ocean acidification assessment in the Iberian upwelling system (1976–2018), Earth Syst. Sci. Data, 12, 2647–2663, https://doi.org/10.5194/essd-12-2647-2020, 2020.

Palacio-Castro, A. M., Enochs, I. C., Besemer, N., Boyd, A., Jankulak, M., Kolodziej, G., Hirsh, H. K., Webb, A. E., Towle, E. K., Kelble, C., Smith, I., and Manzello, D. P.: Coral reef carbonate chemistry reveals interannual, seasonal, and spatial impacts on ocean acidification off Florida, Global Biogeochem. Cy., 37, e2023GB007789, https://doi.org/10.1029/2023GB007789, 2023.

Pardo, P. C., Tilbrook, B., Langlais, C., Trull, T. W., and Rintoul, S. R.: Carbon uptake and biogeochemical change in the Southern Ocean, south of Tasmania, Biogeosciences, 14, 5217–5237, https://doi.org/10.5194/bg-14-5217-2017, 2017.

Pérez, F. F., Becker, M., Goris, N., Gehlen, M., López-Mozos, M., Tjiputra, J., Olsen, A., Müller, J. D., Huertas, I. E., Chau, T. T. T., Cainzos, V., Velo, A., Benard, G., Hauck, J., Gruber, N., and Wanninkhof, R.: An assessment of CO_2 storage and sea-air fluxes for the Atlantic Ocean and Mediterranean Sea between 1985 and 2018, Global Biogeochem. Cy., 38, e2023GB007862, https://doi.org/10.1029/2023GB007862, 2024.

Petton, S., Pernet, F., Le Roy, V., Huber, M., Martin, S., Macé, É., Bozec, Y., Loisel, S., Rimmelin-Maury, P., Grossteffan, É., Repecaud, M., Quemener, L., Retho, M., Manac'h, S., Papin, M., Pineau, P., Lacoue-Labarthe, T., Deborde, J., Costes, L., Polsenaere, P., Rigouin, L., Benhamou, J., Gouriou, L., Lequeux, J.,

Labourdette, N., Savoye, N., Messiaen, G., Foucault, E., Ouisse, V., Richard, M., Lagarde, F., Voron, F., Kempf, V., Mas, S., Gianecchini, L., Vidussi, F., Mostajir, B., Leredde, Y., Alliouane, S., Gattuso, J.-P., and Gazeau, F.: French coastal network for carbonate system monitoring: the CocoriCO_2 dataset, Earth Syst. Sci. Data, 16, 1667–1688, https://doi.org/10.5194/essd-16-1667-2024, 2024.

Poisson, A., Culkin, F., and Ridout, P.: Intercomparison of CO_2 measurements, Deep-Sea Res. Pt. A., 37, 1647–1650, https://doi.org/10.1016/0198-0149(90)90067-6, 1990.

Regnier, P., Friedlingstein, P., Ciais, P., Mackenzie, F. T., Gruber, N., Janssens, I. A., Laruelle, G. G., Lauerwald, R., Luyssaert, S., Andersson, A. J., Arndt, S., Arnosti, C., Borges, A. V., Dale, A. W., Gallego Sala, A., Goddéris, Y., Goossens, N., Hartmann, J., Heinze, C., Ilyina, T., Joos, F., LaRowe, D. E., Leifeld, J., Meysman, F. J. R., Munhoven, G., Raymond, P. A., Spahni, R., Suntharalingam P., and Thullner, M.: Anthropogenic perturbation of the carbon fluxes from land to ocean, Nat. Geosci., 6, 597–607, 2013.

Resplandy, L., Hogikyan, A., Müller, J. D., Najjar, R. G., Bange, H. W., Bianchi, D., Weber, T., Cai, W.-J., Doney, S. C., Fennel, K., Gehlen, M., Hauck, J., Lacroix, F., Landschützer, P., Le Quéré, C., Roobaert, A., Schwinger, J., Berthet, S., Bopp, L., Chau, T. T. T., Dai, M., Gruber, N., Ilyina, T., Kock, A., Manizza, M., Lachkar, Z., Laruelle, G. G., Liao, E., Lima, I. D., Nissen, C., Rödenbeck, C., Séférian, R., Toyama, K., Tsujino, H., and Regnier, P.: A synthesis of global coastal ocean greenhouse gas fluxes, Global Biogeochem. Cy., 38, e2023GB007803, https://doi.org/10.1029/2023GB007803, 2024.

Revelle, R. and Suess, H. E.: Carbon dioxide exchange between atmosphere and ocean and the question of an increase of atmospheric CO_2 during the past decades, Tellus, 9, 18–27, https://doi.org/10.1111/j.2153-3490.1957.tb01849.x, 1957.

Reverdin, G., Metzl, N., Olafsdottir, S., Racapé, V., Takahashi, T., Benetti, M., Valdimarsson, H., Benoit-Cattin, A., Danielsen, M., Fin, J., Naamar, A., Pierrot, D., Sullivan, K., Bringas, F., and Goni, G.: SURATLANT: a 1993–2017 surface sampling in the central part of the North Atlantic subpolar gyre, Earth Syst. Sci. Data, 10, 1901–1924, https://doi.org/10.5194/essd-10-1901-2018, 2018.

Rodgers, K. B., Schwinger, J., Fassbender, A. J., Landschützer, P., Yamaguchi, R., Frenzel, H., Stein, K., Müller, J. D., Goris, N., Sharma, S., Bushinsky, S., Chau, T. T. T., Gehlen, M., Gallego, M. A., Gloege, L., Gregor, L., Gruber, N., Hauck, J., Iida, Y., Ishii, M., Keppler, L., Kim, J.-E., Schlunegger, S., Tjiputra, J., Toyama, K., Ayar, P. V., and Velo, A.: Seasonal variability of the surface ocean carbon cycle: A synthesis, Global Biogeochem. Cy., 37, e2023GB007798, https://doi.org/10.1029/2023GB007798, 2023

Roobaert, A., Resplandy, L., Laruelle, G. G., Liao, E., and Regnier, P.: Unraveling the physical and biological controls of the global coastal CO_2 sink, Global Biogeochem. Cy., 38, e2023GB007799, https://doi.org/10.1029/2023GB007799, 2024a.

Roobaert, A., Regnier, P., Landschützer, P., and Laruelle, G. G.: A novel sea surface pCO_2-product for the global coastal ocean resolving trends over 1982–2020, Earth Syst. Sci. Data, 16, 421–441, https://doi.org/10.5194/essd-16-421-2024, 2024b.

Sarma, V. V. S. S., Krishna, M. S., Paul, Y. S., and Murty, V. S. N.: Observed changes in ocean acidity and carbon dioxide exchange in the coastal bay of Bengal – A link to air pollution, Tellus B, 67, 24638, https://doi.org/10.3402/tellusb.v67.24638, 2015.

Sarma, V. V. S. S., Sridevi, B., Metzl, N., Patra, P. K., Lachkar, Z., Chakraborty, K., Goyet, C., Levy, M., Mehari, M., and Chandra, N.: Air-sea fluxes of CO_2 in the Indian Ocean between 1985 and 2018: A synthesis based on observation-based surface CO_2, hindcast and atmospheric inversion models, Global Biogeochem. Cy., 37, e2023GB007694, https://doi.org/10.1029/2023GB007694, 2023.

Sarmiento, J. L., Johnson, K. S., Arteaga, L. A., Bushinsky, S. M., Cullen, H. M., Gray, A. R., Hotinski, R. M., Maurer, T. L., Mazloff, M. R., Riser, S. C., Russell, J. L., Schofield, O. M., and Talley, L. D.: The Southern Ocean Carbon and Climate Observations and Modeling (SOCCOM) project: A review, Prog. Oceanogr., 2019, 103130, https://doi.org/10.1016/j.pocean.2023.103130, 2023.

Schlitzer, R.: Ocean Data View, Ocean Data View, http://odv.awi.de (last access: 13 March 2019), 2018.

Schneider, A., Wallace, D. W. R., and Körtzinger, A.: Alkalinity of the Mediterranean Sea, Geophys. Res. Lett., 34, L15608, https://doi.org/10.1029/2006GL028842, 2007.

Schuster, U., McKinley, G. A., Bates, N., Chevallier, F., Doney, S. C., Fay, A. R., González-Dávila, M., Gruber, N., Jones, S., Krijnen, J., Landschützer, P., Lefèvre, N., Manizza, M., Mathis, J., Metzl, N., Olsen, A., Rios, A. F., Rödenbeck, C., Santana-Casiano, J. M., Takahashi, T., Wanninkhof, R., and Watson, A. J.: An assessment of the Atlantic and Arctic sea–air CO2 fluxes, 1990–2009, Biogeosciences, 10, 607–627, https://doi.org/10.5194/bg-10-607-2013, 2013.

Shadwick, E., Rintoul, S., Tilbrook, B., Williams, G., Young, N., Fraser, A. D., Marchant, H., Smith, J., and Tamura, T.: Glacier tongue calving reduced dense water formation and enhanced carbon uptake, Geophys. Res. Lett., 40, 904–909, https://doi.org/10.1002/grl.50178, 2013.

Shadwick, E. H., Tilbrook, B., and Williams, G. D.: Carbonate chemistry in the Mertz Polynya (East Antarctica): Biological and physical modification of dense water outflows and the export of anthropogenic CO_2, J. Geophys. Res. Oceans, 119, 1–14, https://doi.org/10.1002/2013JC009286, 2014.

Shadwick, E. H., Trull, T. W., Tilbrook, B., Sutton, A. J., Schulz, E., and Sabine, C. L.: Seasonality of biological and physical controls on surface ocean CO_2 from hourly observations at the Southern Ocean Time Series site south of Australia, Global Biogeochem. Cy., 29, 223–238, https://doi.org/10.1002/2014GB004906, 2015.

Shadwick, E. H., Wynn-Edwards, C. A., Matear, R. J., Jansen, P., Schulz, E., and Sutton, A. J.: Observed amplification of the seasonal CO_2 cycle at the Southern Ocean Time Series, Front. Mar. Sci., 10, 1281854, https://doi.org/10.3389/fmars.2023.1281854, 2023.

Siddiqui, A. H., Haine, T. W. N., Nguyen, A. T., and Buckley, M. W.: Controls on upper ocean salinity variability in the eastern subpolar North Atlantic during 1992–2017, J. Geophys. Rese.-Oceans, 129, e2024JC020887, https://doi.org/10.1029/2024JC020887, 2024.

SNAPO-CO2: ODV collection, https://explore.webodv.awi.de/ocean/carbon/snapo-co2/ (last access: 22 January 2025), 2024.

Sridevi, B. and Sarma, V. V. S. S.: Role of river discharge and warming on ocean acidification and pco2 levels in the Bay of Bengal, Tellus B, 73, 1–20, https://doi.org/10.1080/16000889.2021.1971924, 2021.

Sutton, A. J., Battisti, R., Carter, B., Evans, W., Newton, J., Alin, S., Bates, N. R., Cai, W.-J., Currie, K., Feely, R. A., Sabine, C., Tanhua, T., Tilbrook, B., and Wanninkhof, R.: Advancing best practices for assessing trends of ocean acidification time series. Frontiers in Marine Science, 9: 1045667. https://doi.org/10.3389/fmars.2022.1045667, 2022

Takahashi, T., Sutherland, S. C., Wanninkhof, R., Sweeney, C., Feely, R. A., Chipman, D. W., Hales, B., Friederich, G., Chavez, F., Sabine, C., Watson, A. J., Bakker, D. C., Schuster, U., Metzl, N., Yoshikawa-Inoue, H., Ishii, M., Midorikawa, T., Nojiri, Y., Körtzinger, A., Steinhoff, T., Hoppema, M., Olafsson, J., Arnarson, T. S., Tilbrook, B., Johannessen, T., Olsen, A., Bellerby, R., Wong, C., Delille, B., Bates, N., and de Baar, H. J.: Climatological mean and decadal change in surface ocean pCO_2, and net sea air CO_2 flux over the global oceans, Deep-Sea Res. Pt. II, 56, 554–577, https://doi.org/10.1016/j.dsr2.2008.12.009, 2009.

Takahashi, T., Sutherland, S. C., Chipman, D. W., Goddard, J. G., Ho, C., Newberger, T., Sweeney, C. and Munro, D. R.: Climatological distributions of pH, pCO_2, total CO_2, alkalinity, and $CaCO_3$ saturation in the global surface ocean, and temporal changes at selected locations, Mar. Chem., 164, 95–125, https://doi.org/10.1016/j.marchem.2014.06.004, 2014.

Ternon, J.-F., Oudot, C., Dessier, A., and Diverres, D.: A seasonal tropical sink for atmospheric CO_2 in the Atlantic ocean: the role of the Amazon River discharge, Mar. Chem., 68, 183–201, https://doi.org/10.1016/S0304-4203(99)00077-8, 2000.

Thomas, H., Prowe, A. E. F., Lima, I. D., Doney, S. C., Wanninkhof, R., Greatbatch, R. J., Schuster, U., and Corbière, A.: Changes in the North Atlantic Oscillation influence CO_2 uptake in the North Atlantic over the past 2 decades, Global Biogeochem. Cy., 22, GB4027, https://doi.org/10.1029/2007GB003167, 2008.

Tilbrook, B., Jewett, E. B., DeGrandpre, M. D., Hernandez-Ayon, J. M., Feely, R. A., Gledhill, D. K., Hansson, L., Isensee, K., Kurz, M. L., Newton, J. A., Siedlecki, S. A., Chai, F., Dupont, S., Graco, M., Calvo, E., Greeley, D., Kapsenberg, L., Lebrec, M., Pelejero, C., Schoo, K. L., and Telszewski, M.: An Enhanced Ocean Acidification Observing Network: From People to Technology to Data Synthesis and Information Exchange, Front. Mar Sci., 6, 337, https://doi.org/10.3389/fmars.2019.00337, 2019.

Touratier, F. and Goyet, C.: Decadal evolution of anthropogenic CO_2 in the north western Mediterranean Sea from the mid-1990's to the mid-2000's, Deep-Sea Res. Pt. I, 56, 1708–1716, https://doi.org/10.1016/j.dsr.2009.05.015, 2009.

Ulses, C., Estournel, C., Fourrier, M., Coppola, L., Kessouri, F., Lefèvre, D., and Marsaleix, P.: Oxygen budget of the north-western Mediterranean deep- convection region, Biogeosciences, 18, 937–960, https://doi.org/10.5194/bg-18-937-2021, 2021.

Ulses, C., Estournel, C., Marsaleix, P., Soetaert, K., Fourrier, M., Coppola, L., Lefèvre, D., Touratier, F., Goyet, C., Guglielmi, V., Kessouri, F., Testor, P., and Durrieu de Madron, X.: Seasonal dynamics and annual budget of dissolved inorganic carbon in the northwestern Mediterranean deep-convection region, Biogeosciences, 20, 4683–4710, https://doi.org/10.5194/bg-20-4683-2023, 2023.

UNESCO: Intercomparison of total alkalinity and total inorganic carbon determinations in seawater, UNESCO Tech. Pap. Mar. Sci., 59, https://www.jodc.go.jp/jodcweb/info/ioc_doc/UNESCO_tech/090199eb.pdf (last access: 22 December 2023), 1990.

UNESCO: Reference materials for oceanic carbon dioxide measurements, UNESCO Tech. Pap. Mar. Sci., 60, https://www.jodc.go.jp/jodcweb/info/ioc_doc/UNESCO_tech/090200eb.pdf (last access: 22 December 2023), 1991.

Vance, J. M., Currie, K., Suanda, S. H., and Law, C. S.: Drivers of seasonal to decadal mixed layer carbon cycle variability in subantarctic water in the Munida Time Series, Front. Mar. Sci., 11, 1309560, https://doi.org/10.3389/fmars.2024.1309560, 2024.

von Schuckmann, K., Minière, A., Gues, F., Cuesta-Valero, F. J., Kirchengast, G., Adusumilli, S., Straneo, F., Ablain, M., Allan, R. P., Barker, P. M., Beltrami, H., Blazquez, A., Boyer, T., Cheng, L., Church, J., Desbruyeres, D., Dolman, H., Domingues, C. M., García-García, A., Giglio, D., Gilson, J. E., Gorfer, M., Haimberger, L., Hakuba, M. Z., Hendricks, S., Hosoda, S., Johnson, G. C., Killick, R., King, B., Kolodziejczyk, N., Korosov, A., Krinner, G., Kuusela, M., Landerer, F. W., Langer, M., Lavergne, T., Lawrence, I., Li, Y., Lyman, J., Marti, F., Marzeion, B., Mayer, M., MacDougall, A. H., McDougall, T., Monselesan, D. P., Nitzbon, J., Otosaka, I., Peng, J., Purkey, S., Roemmich, D., Sato, K., Sato, K., Savita, A., Schweiger, A., Shepherd, A., Seneviratne, S. I., Simons, L., Slater, D. A., Slater, T., Steiner, A. K., Suga, T., Szekely, T., Thiery, W., Timmermans, M.-L., Vanderkelen, I., Wjiffels, S. E., Wu, T., and Zemp, M.: Heat stored in the Earth system 1960–2020: where does the energy go?, Earth Syst. Sci. Data, 15, 1675–1709, https://doi.org/10.5194/essd-15-1675-2023, 2023.

Wagener, T., Metzl, N., Caffin, M., Fin, J., Helias Nunige, S., Lefevre, D., Lo Monaco, C., Rougier, G., and Moutin, T.: Carbonate system distribution, anthropogenic carbon and acidification in the western tropical South Pacific (OUTPACE 2015 transect), Biogeosciences, 15, 5221–5236, https://doi.org/10.5194/bg-15-5221-2018, 2018.

Wimart-Rousseau, C., Lajaunie-Salla, K., Marrec, P., Wagener, T., Raimbault, P., Lagadec, V., Lafont, M., Garcia, N., Diaz, F., Pinazo, C., Yohia, C., Garcia, F., Xueref-Remy,I., Blanc, P.-E., Armengaud, A., and Lefèvre, D.: Temporal variability of the carbonate system and air-sea CO_2 exchanges in a Mediterranean human-impacted coastal site, Estuar. Coast. Shelf S., 236, 106641, https://doi.org/10.1016/j.ecss.2020.106641, 2020.

Wimart-Rousseau, C., Wagener, T., Bosse, A., Raimbault, P., Coppola, L., Fourrier, M., Ulses, C., and Lefèvre, D.: Assessing seasonal and interannual changes in carbonate chemistry across two timeseries sites in the North Western Mediterranean Sea., Front. Mar. Sci., 10, 1281003, https://doi.org/10.3389/fmars.2023.1281003, 2023.

WMO/GCOS: Global Climate Indicators, https://gcos.wmo.int/en/global-climate-indicators (last access: 22 December 2023), 2018.

Yao, M. K., Marcou, O., Goyet, C., Guglielmi, V., Touratier, F., and Savy, J.-P.: Time variability of the north-western Mediterranean Sea pH over 1995–2011, Mar. Environ. Res., 116, 51–60, https://doi.org/10.1016/j.marenvres.2016.02.016, 2016.

Yoder, M. F., Palevsky, H. I., and Fogaren, K. E.: Net community production and inorganic carbon cycling in the central

Irminger Sea, J. Geophys. Res.-Oceans, 129, e2024JC021027, https://doi.org/10.1029/2024JC021027, 2024.

Zhang, S., Wu, Y., Cai, W.-J., Cai, W., Feely, R. A., Wang, Z., Tanhua, T., Wang, Y., Liu, C., Li, X., Yang, Q., Ding, M., Xu, Z., Kerr, R., Luo, Y., Cheng, X., Chen, L., and Qi, D.: Transport of anthropogenic carbon from the Antarctic shelf to deep Southern Ocean triggers acidification, Global Biogeochem. Cy., 37, e2023GB007921, https://doi.org/10.1029/2023GB007921, 2023.